Published in final edited form as:

Dev Genes Evol. 2018 January ; 228(1): 31–48. doi:10.1007/s00427-017-0601-8.

Two Drosophilids exhibit distinct EGF-pathway patterns in oogenesis

Kenley N. O'Hanlon[*,1], **Rachel A. Dam**[*,2], **Sophie L. Archambeault**[2,3], and **Celeste A. Berg**[†,1,2]

[1]Department of Genome Sciences, 3720 15th AVE NE, University of Washington, Seattle, WA 98195-5065 [2]Molecular and Cellular Biology Program, 1959 NE Pacific Street, University of Washington, Seattle, WA 98195-7275 [3]Current Address, Institute of Ecology and Evolution, University of Bern, Baltzerstrasse 6, 3012 Bern, Switzerland

Abstract

Deciphering the evolution of morphological structures is a remaining challenge in the field of developmental biology. The respiratory structures of insect eggshells, called the dorsal appendages, provide an outstanding system for exploring these processes since considerable information is known about their patterning and morphogenesis in *Drosophila melanogaster*, and dorsal appendage number and morphology vary widely across Drosophilid species. We investigated the patterning differences that might facilitate morphogenetic differences between *D. melanogaster*, which produces two oar-like structures first by wrapping and then elongating the tubes via cell intercalation and cell crawling, and *Scaptodrosophila lebanonensis*, which produces a variable number of appendages simply by cell intercalation and crawling. Analyses of BMP-pathway components *thickveins* and P-Mad demonstrate that anterior patterning is conserved between these species. In contrast, EGF signaling exhibits significant differences. Transcripts for the ligand encoded by *gurken* localize similarly in the two species, but this morphogen creates a single dorsolateral primordium in *S. lebanonensis* as defined by activated MAP kinase and the downstream marker *broad*. Expression patterns of *pointed, argos*, and Capicua, early steps in the EGF pathway, exhibit a heterochronic shift in *S. lebanonensis* relative to those seen in *D. melanogaster*. We demonstrate that the *S. lebanonensis* Gurken homolog is active in *D. melanogaster* but is insufficient to alter downstream patterning responses, indicating that Gurken-EGF receptor interactions do not distinguish the two species' patterning. Altogether, these results differentiate EGF signaling patterns between species and shed light on how changes to the regulation of patterning genes may contribute to different tube- forming mechanisms.

[†]Corresponding Author: caberg@uw.edu 206-543-1677.
[*]These authors contributed equally to this manuscript.

ORCID IDs
Rachel Dam: orcid.org/0000-0002-6740-8065
Sophie Archambeault: orcid.org/0000-0001-9409-7541
Celeste Berg: orcid.org/0000-0002-2605-1768

The authors declare no competing interests.

Keywords

Dorsal appendages; Scaptodrosophila; Drosophila; follicle cells; eggshell; epithelial morphogenesis

Introduction

Tube formation is an important developmental process since tubes let us eat, breathe, transport nutrients, discard waste materials, and exchange gametes. Tube formation can occur through many routes; for example, pre-existing epithelial sheets can be transformed into tubes through budding or wrapping, while clusters of non-epithelial cells can be converted into epithelial tubes through cavitation and cord hollowing (Lubarsky and Krasnow 2003). One example of epithelial tubulogenesis is the formation of the insect eggshell specializations called dorsal appendages (DAs). DAs are proteinaceous structures that reside at the dorsal anterior end of the mature eggshell and facilitate gas exchange for the developing embryo (Hinton, 1960). Recent work has unexpectedly shown that different cellular mechanisms produce homologous DA structures in different species (Osterfield et al. 2015). This finding highlights a gap in our understanding of how gene expression and morphogenesis interact to shape functional morphology over relatively short evolutionary distances. To investigate the morphogenetic basis for the diversity of tube-forming mechanisms across species, we compared gene expression patterns during DA formation in *Drosophila melanogaster* and *Scaptodrosophila lebanonensis*.

DA formation occurs during oogenesis, which is well characterized in *D. melanogaster* (King 1970; Spradling 1993; Hudson and Cooley 2014). The units of development are the egg chambers, which develop in assembly lines called ovarioles. In *D. melanogaster*, each ovariole contains 6–7 egg chambers in progressive stages of oogenesis (Fig. A1a) (Horne-Badovinac and Bilder 2005), and each ovary contains approximately 13–30 ovarioles (Lobell et al. 2017). Ovary development begins in the late third larval instar, and the first egg chambers appear about 3 days later during pupal development. Egg chambers then mature through 14 morphologically distinct stages (S1–S14), a process that requires an additional 70 to 96 hours (King 1970; Lin and Spradling 1993). Thus, ovaries from a newly-eclosed female have a range of egg chamber stages up to S6 or S7, and two days later, ovaries from a well-fed female contain all stages of oogenesis including mature eggs ready to be fertilized and laid (Fig. A1c).

Oogenesis in *S. lebanonensis* produces similarly distinct stages, but egg chamber production differs substantially. Ovarioles usually contain only 2–3 egg chambers that develop synchronously between ovarioles and, as a result, only a few stages are present in a single *S. lebanonensis* ovary (Fig. A1b). In addition, *S. lebanonensis* ovaries either start developing slightly later than *D. melanogaster* ovaries and/or require a longer period for each stage. Egg chambers from newly eclosed females are just emerging from the germarium and therefore do not reach maturity until 3 days after eclosion (Fig. A1c).

Egg chambers consist of 16 germline-derived cells (the oocyte and 15 polyploid nurse cells) that are surrounded by a single-cell-thick layer of somatic follicle cells. At stage S10B,

when DA formation begins, the oocyte occupies the posterior half of the egg chamber and the nurse cells occupy the anterior half. At this time, the follicle cells are divided into two categories: ~ 50 follicle cells (the stretch cells) form a squamous layer over the nurse cells while ~ 600 follicle cells form a columnar layer over the oocyte. A subset of columnar cells eventually gives rise to the DAs.

The morphologically distinct DAs of *D. melanogaster* and *Scaptodrosophila* flies are produced by different cellular mechanisms within the egg chamber. In *Drosophila melanogaster*, two patches of dorsal anterior follicle cells "wrap" to form two small, nub-like tubes parallel to the epithelial sheet. The cells in these DA primordia then change shape and intercalate, elongating the tubes to create oar-like structures with a rounded stalk and flattened paddle. Concurrent with these dramatic cellular changes, the follicle cells secrete chorionic eggshell protein into the lumen of the tubes (reviewed by Osterfield et al. 2017). Although the follicle cells slough off when the egg is laid, the resultant DA morphology is a direct readout of how morphogenesis proceeded (Fig. 1a, b). In contrast, *Scaptodrosophila pattersoni* lacks the canonical wrapping mechanism that occurs in *D. melanogaster* during DA formation. Instead, groups of follicle cells simply extend toward the anterior to make 5–8 long, thin DAs (Osterfield et al. 2015). This unexpected mechanism also operates in *Scaptodrosophila lebanonensis* to form 4–8 DAs (Fig. 1d–f). Phylogenetic evidence (Bächli et al. 2005) and single-pair interspecies matings (see methods) suggest that the two strains are the same species. Since a draft genome for *S. lebanonensis* is available on NCBI (Vicoso and Bachtrog 2015), we focused our analyses on this strain.

In *D. melanogaster*, two signaling pathways combine to specify the DA primordia; epidermal growth factor (EGF) signals originate from the oocyte, and bone morphogenetic protein (BMP) originates from the squamous stretch follicle cells (Fig. 1c) (Berg 2005). The *broad* gene (*br*), which encodes several zinc-finger transcription factors (DiBello et al. 1991), integrates these signals (Deng and Bownes 1997) and through feed-forward and feedback loops, defines two cell types, called floor and roof cells. These two cell types cooperate to make the DA tubes (reviewed by Osterfield et al. 2017; and Pyrowolakis et al. 2017).

The EGF signal, a TGF-α like ligand encoded by *gurken* (*grk*), is a morphogen; different levels either activate or inhibit *br* expression (Fig. 1c) (Goentoro et al. 2006). High levels of Grk inhibit DA-forming fate through the activity of *pointed* (*pnt*), which encodes two ETS-like transcription factors that repress *br* expression (Morimoto et al. 1996). The proteins' common region includes the 3 exons that comprise the ETS domain but are distinguished in part by their respective promoter regions (*P1* and *P2*), which are ~ 50 kb apart (Klämbt 1993; O'Neill et al. 1994). High levels of Grk also induce expression of a secreted inhibitor encoded by *argos* (*aos*) (Golembo et al. 1996; Wasserman and Freeman 1998; Klein et al. 2004). Although Aos is not necessary for DA-tube-cell fate (Boisclaire Lachance et al. 2009), in this developmental context *aos* expression resembles *pnt* expression and is a good marker for *br* inhibition. In response to moderate levels of Grk (Fig. 1c), EGF activation no longer reaches the threshold for expression of *pnt* and *aos*; instead, other pathway components activate *br* expression, in part through down-regulation of the HMG-box protein Capicua (Cic) (Goff et al. 2001; Astigarraga et al. 2007). Cic is normally found in follicle

cell nuclei where it represses the homeobox gene *mirror* (*mirr*) (Atkey et al. 2006; Astigarraga et al. 2007). Phosphorylation of Cic by Egfr-activated MAPK causes the protein to accumulate in the cytoplasm (Astigarraga et al. 2007), allowing Mirr to activate *br* and define the DA roof cells (Astigarraga et al. 2007; Fuchs et al. 2012).

While the EGF pathway determines DA tube-cell fate in a feed-forward manner, the BMP2/4-like ligand, Decapentaplegic (Dpp), contributes to patterning in a negative feedback loop with Broad (Twombly et al. 1996; Peri and Roth 2000; Yakoby et al. 2008). Broad induces expression of *thickveins* (*tkv*), which encodes one of the type I Dpp receptors (Mantrova et al. 1999; Lembong et al. 2008; Yakoby et al. 2008). In response to Dpp ligand-receptor binding, Mothers against dpp (Mad), a Smad protein, is phosphorylated (P-Mad). The activated protein then inhibits Br in anterior cells, defining the "centripetally-migrating cells" that form the operculum of the mature eggshell (Dobens et al. 2000). Over time, P-Mad activity expands posteriorly, first repressing *br* in the floor cells, and later down-regulating *br* transcription in roof cells (Yakoby et al. 2008).

Together, the EGF and BMP pathways pattern the DA primordia in *D. melanogaster* and presumably also in *S. lebanonensis*. Given the unexpected differences in the cellular mechanisms driving DA formation in *D. melanogaster* and *S. lebanonensis*, we questioned whether the EGF and BMP pathways pattern the DA primordia in *S. lebanonensis* in the same way. We therefore characterized EGF and BMP pathway components in *S. lebanonensis* and ascertained the extent to which patterning differences contribute to different eggshell morphologies.

Methods

Fly Stocks, Crosses, and Maintenance

S. lebanonensis was obtained from the *Drosophila* Species Stock Center (#11010-0021.00). *MTD-Gal4* (Petrella et al. 2007) is available from the Bloomington Stock Center (#31777) and is described in FlyBase (http://flybase.org). *UASp-grk.mb* was a gift from N. Perrimon (Ghiglione et al. 2002). Flies were maintained on standard cornmeal molasses medium.

To test species relatedness of *S. lebanonensis* and *S. pattersoni*, newly eclosed virgin females and males were collected for each species and aged separately for four days at 25°C. 40 single-pair matings were established: 10 *S. pattersoni* females x *S. lebanonensis* males, 10 *S. lebanonensis* females x *S. pattersoni* males, and 10 intra-species matings for each strain as controls. All crosses yielded > 50 progeny, except one *S. lebanonensis* x *S. lebanonensis* control, which produced only 10 offspring. Female and male F1 hybrids from each cross were tested for fertility by sibling matings and all hybrids were fertile.

Egg Collections and Eggshell Imaging

Transgenic flies were reared and crosses set up at 25°. For the egg collections, 25 female flies and 15 w^{1118} males were aged 1 day at 25°, then placed at 18°C, 22°C, 25°C, or 30°C for 1 day before transferring to egg collection bottles containing apple juice plates with a dab of wet yeast paste. Flies were maintained at the specified temperature for 48 hours prior to collecting eggs. Plates were changed daily. Eggs were mounted in Hoyer's mounting

medium (van der Meer 1977). Images were acquired using darkfield optics on a LaboPhot-2 microscope (Nikon) connected to a digital MU1300 camera (AmScope) and processed using Helicon Focus (Helicon Soft).

Cloning of S. lebanonensis gurken *cDNA*

Total RNA was isolated from *S. lebanonensis* ovaries using the RNAqueous-4PCR Total RNA Isolation kit (ThermoFisher). cDNA was generated with the Transcriptor High Fidelity cDNA Synthesis Kit (Roche) using the primers 5′-ATACGTACGATCAGGGGACA-3′ (FW) and 5′- TCTTCAGCCAAACCCAGTTC-3′ (REV), which bracket the 5′UTR, coding sequence, and most of the 3′UTR from *S. lebanonensis grk.* The grk^{SI} cDNA was amplified and then ligated into the $BamH_I$ and Xba_I sites of the *pUASp-attB* plasmid (Stock #1358, *Drosophila* Genomics Resource Center). Sequence-verified *pUASp-Sleb-grk* plasmid was sent to Rainbow Transgenics for injection. The transgene was inserted in *D. melanogaster* on chromosome arm 3L at 68A4, *attP2* (Bloomington Stock #25710).

RNA probe generation

Probe generation was carried out as described previously (Zimmerman et al. 2013).

D. melanogaster Probes

D. melanogaster aos and *pnt* probes were generated from cDNA constructs obtained from the Drosophila Genomics Resources Center (DGRC). *aos* was generated from the entire 3.0-kb insert of RE21614, and *pnt* from an amplified region of RE52147. The primers 5′-AACATACTGATTGTCGCGCG-3′ (FW) and 5′-TGGCTATGCATCTACGAGCT-3′ (REV) were used to amplify a 1.6-kb common region shared by both *pnt* transcripts, *P1* and *P2*.

D. melanogaster tkv probes were generated from genomic DNA obtained from adult Canton S flies. Primers 5′-CGCTCCCTAACCTGCTACTG-3′ (FW) and 5′-CTCCTGTCTGTTGGCTCCTG-3′ (REV) were used to amplify a 2.2-kb region that included most of the last two exons and part of the 3′UTR of *tkv* transcripts.

D. melanogaster grk and *br* probes were those generated and used in (Zimmerman et al. 2013). *grk* was generated from the complete 1.7-kb cDNA (GenBank ID: L22531) construct described in (Neuman-Silberberg and Schüpbach 1993). *br* was generated from genomic DNA obtained from Canton S flies. Primers 5′-GCCCTGGTGGAGT-3′ (FW) and 5′-GCGTTAGTTGGTC-3′ (REV) were used to amplify a 1.3-kb region encoding the conserved Bric-a-brac–Tramtrack–Broad dimerization domain present in all known *D. melanogaster broad* transcripts.

S. lebanonensis Probes

All *S. lebanonensis* probes were designed using genomic sequences from

Scaptodrosophila lebanonensis (taxid:7225; Vicoso and Bachtrog 2015). Orthologous genes were identified by NCBI tBLASTn using *D. melanogaster* protein sequences.

grk – Scaffold 12493: The amplified fragment was designed to hybridize to the last two Grk coding exons and part of the 3′ UTR: 5′-AGCACACGCTGAAAATTGTG-3′ (FW); 5′-GGTTGGCAACGCTTTGTTAT-3′ (REV); 1.5 kb

pnt – Scaffold 26438: Due to the short protein-coding exons associated with the *P1* and *P2* transcripts, and to the draft nature of the *S. lebanonensis* genome assembly, we were unable to identify the unique regions that specified the *P1* and *P2* transcripts. The amplified fragment was designed to hybridize to a conserved common region present in both transcripts: 5′-GCAGGAGCATCAGAGTCAGG-3′ (FW); 5′-GATCGCAGGTTATGCTGCTT-3′ (REV); 1.9 kb

aos – Scaffold 23624: The amplified fragment was designed to hybridize within the second Aos coding exon: 5′-GAAACGCCTTGGATCGAGC-3′ (FW); 5′-TGCAAACAGGGAGCTTGTG-3′ (REV); 0.5 kb

tkv – Scaffold 6086: The amplified fragment was designed to hybridize to the last Tkv coding exon, which is present in all known *D. melanogaster* transcripts: 5′-CATGGCAAGAACATCGTTTG-3′ (FW); 5′-ATAGTCCTCGCAGGTGGTTG-3′ (REV); 1.0 kb

br – Scaffold 12319: The amplified fragment was designed to hybridize to two exons that encode the conserved Bric-a-brac–Tramtrack–Broad dimerization domain present in all known *D. melanogaster broad* transcripts: 5′-CTGCACTCGCTGGTCGAAT-3′ (FW); 5′-CTGCTAGAGCGATTGGCATC-3′ (REV); 1.0 kb

Preparation of ovaries for in situ hybridization, immunostaining, and IF/FISH

1-day old *D. melanogaster* flies were supplied with males and wet yeast for 2 days at 25°C and then dissected. To obtain all oogenesis stages on the same day of dissection for *S. lebanonensis*, we manipulated adult females using a combination of environmental regimes. Newly-eclosed *S. lebanonensis* females were allocated into four groups, and each group was mated and supplied with wet yeast. The four groups were placed at 22°C for 3 days (S11–14), 25°C for 2 days (S6–9), 25°C for 3 days (S14, S1–6), and 30°C for 2 days (S8–10).

RNA in situ hybridization (ISH)

D. melanogaster ovaries underwent the optimized ISH protocol (Zimmerman et al. 2013). *S. lebanonensis* ovaries underwent an adapted form of the protocol in which the RNase inactivation step immediately followed the primary fixation step. For all samples, sense and anti-sense probes were calibrated by dot blot and diluted to be of equal concentration. Matched probes were hybridized using 1:500 dilution.

Immunostaining and Dual ImmunoFluorescence and Fluorescent in situ Hybridization (IF/FISH)

Immunostaining and IF/FISH were carried out as described previously (Zimmerman et al. 2013). Primary antibodies used were: mouse anti-Broad core (Developmental Studies Hybridoma Bank [DSHB] 25E9.D7-concentrate, 1:500); rat anti-DE-cadherin (DSHB DCAD2- concentrate, 1:50); mouse anti-Gurken (DSHB 1D12-concentrate, 1:200); rabbit

anti-Capicua (Kim et al. 2011, 1:2000 in *D. melanogaster;* 1:500 in *S. lebanonensis*); rabbit anti-P-Mad (a gift from T. Jessell's lab; 1:2000 in both species); rabbit anti-dpERK (Cell Signaling, 1:100). Alexafluor 488-, 568-, and 647-conjugated secondary antibodies (Molecular Probes/Invitrogen) were used at dilutions between 1:200 and 1:500. DAPI was used at a concentration of 1 αg/ml. Probes for FISH were diluted 1:500 in HYB mix.

Microscopy and Imaging

All colorimetric *in situ* hybridization images were obtained using a Nikon Microphot-FXA microscope with a 20X (0.75 NA) objective and an AmScope MU1203-FL digital camera. Multiple focal planes of the sample were imaged and then merged using Helicon Focus (Helicon Soft). Fluorescent images for Fig. A1 were taken using a Zeiss Axioplan 2 with a 5X (0.15 NA) objective. All other fluorescent images were acquired on a Leica SP8X scanning confocal microscope with a 40X (1.30 NA) oil immersion objective. Images were processed using FIJI (ImageJ-based, NIH, Schneider et al. 2012), and displayed as maximum intensity projections.

Results

S. lebanonensis egg chambers define a single, dorsolateral DA primoridum

The transcription factor Broad (Br) delineates the roof cells of the dorsal appendage tubes (Dorman et al. 2004). In earlier stages of oogenesis, from S6–S10A, *br* transcript and protein are expressed in all follicle cells, but at the S10A–S10B transition, both gene products are rapidly down-regulated in a T-shaped pattern of dorsal-anterior follicle cells (Deng and Bownes 1997; Tzolovosky et al. 1999; Yakoby et al. 2008). Then, at S10B, expression in the posterior columnar cells gradually diminishes while two dorsolateral patches up-regulate *br* expression (Fig. 2a) (Cheung et al. 2013).

If patterning in *S. lebanonensis* were similar to that in *D. melanogaster*, egg chambers would exhibit a variable number of *br*-expressing patches. Based on cell shape and behavior, however, Osterfield and colleagues (2015) postulated that there is instead a single dorsolateral band of roof cells that will produce the varying numbers of dorsal appendages. To distinguish between these possibilities, we cloned a region of the *S. lebanonensis br* gene, a region that is common to all known transcripts in *D. melanogaster*, and ascertained the expression pattern of *br* using *in situ* hybridization. Consistent with Miriam Osterfield's morphological studies, S10B egg chambers exhibited *br* expression in a band across the dorsal side of the egg chambers (Fig. 2b, c). The band is approximately 4 cell rows posterior from the oocyte's anterior cortex, and 6 rows of cells wide, as determined by fluorescent *in situ* hybridization (data not shown). The spatial and temporal expression at earlier and later stages are similar to that in *D. melanogaster:, S. lebanonensis br* mRNA is present in all follicle cells from S6 until S10A, when distinct up-regulation occurs at S10B; the transcripts are then degraded by S12 (Fig. A2a–c).

To understand how the *br* expression pattern might differ so much in *S. lebanonensis* at S10B, we examined expression of *gurken*, which initiates all processes upstream of *br.*

gurken patterning is similar between the two species

In *D. melanogaster, grk* mRNA localizes to the posterior of the oocyte during early stages of oogenesis (Neuman-Silberberg and Schüpbach 1993). During mid-oogenesis, *grk* transcripts follow the oocyte nucleus as it migrates to the dorsal anterior corner of the oocyte; *grk* mRNA becomes localized in a cap around the anterior and dorsal sides of the oocyte nucleus and remains there throughout later stages of oogenesis (Fig. 2d; Neuman-Silberberg and Schüpbach 1993). Since *grk* dosage levels affect *br* patterning and dorsal-appendage cell fate (Deng and Bownes 1997; Neuman-Silberberg and Schüpbach 1994), and medium levels initiate *br* activation and create the two DA primordia, we hypothesized that *S. lebanonensis grk* would be present at moderate levels in an extended dorsolateral area at the anterior of the oocyte.

Surprisingly, *in situ* hybridization demonstrated that *grk* expression in *S. lebanonensis* was similar to that of *D. melanogaster.* At S10B, the transcripts were localized tightly around the oocyte nucleus (Fig. 2e) in approximately 60% of S10B egg chambers, while the other 40% of egg chambers maintained a nuclear association with a slight lateral expansion (Fig. 2f, A2i). Like *D. melanogaster*, earlier *S. lebanonensis* stages expressed *grk* at the oocyte posterior, the transcripts migrated to the anterior at S6–S8, and they remained in a cap around the oocyte nucleus in mid-late oogenesis (Fig. A2d–j).

Although we found a slight expansion of *grk* localization relative to patterns seen in *D. melanogaster*, this subtle difference in *grk* expression is not sufficient to explain the large difference in expression of the downstream element of the pathway, *br*.

broad-inhibiting elements are expressed in unexpected regions

To investigate other factors that might produce the observed differences in *br* expression between species, we analyzed the expression of *pointed* (*pnt)* and *argos* (*aos)*. In *D. melanogaster*, two *pnt* transcripts exist in the follicle cells at the anterior and posterior of the oocyte (Morimoto et al. 1996). The *P1* transcript appears at the posterior beginning at S5; at the transition from S10A to S10B, *P1* mRNA also appears in the dorsal anterior corner in a T- shaped pattern of cells that will make the operculum. These patterns refine into two distinct lateral patches at late S10B/S11 (Morimoto et al. 1996). The *P2* transcript is present in a band at the anterior of the oocyte during early oogenesis and then in two dorsolateral patches during late oogenesis (Morimoto et al. 1996). While the *P1*- and *P2*-transcript patterns are dynamic throughout oogenesis, ultimately by S11 they are both expressed in the DA-forming cells where they down-regulate *br* expression (Morimoto et al. 1996). We confirmed these expression patterns in *D. melanogaster* with a probe that hybridizes to the common region of both transcripts (Fig. 3a, b).

We visualized *pnt* expression in *S. lebanonensis* with an *in situ* probe designed to hybridize to a conserved common region of the putative *pnt* transcripts. We observed *pnt* expression at the posterior, similar to *D. melanogaster*, as well as at the anterior (Fig. 3c–e). Unexpectedly, the anterior expression pattern was not in the anterior-most rows of cells, but rather, was shifted slightly more posteriorly to a dorsolateral band 2–3 cells wide at S9; the expression expanded to more rows of cells at S10B (Fig. 3d, e, A3a, b). By S12, anterior expression

disappeared and transcripts were present only at the posterior (Fig. A3c). Based on the transcript pattern at S10B, we speculate that *pnt* localization overlaps with *br* expression. Thus, *pnt* expression in *S. lebanonensis* more closely aligns with the late (S11) *pnt* expression patterns in *D. melanogaster* rather than the earlier midline "T" pattern where Pnt functions to inhibit DA-cell specification.

To explore this result more fully, we examined a second midline marker, *aos.* In *D. melanogaster, aos* is expressed in a T-shaped domain at the midline in S11 egg chambers (Fig. 3f). In later stage egg chambers, the pattern refines to two eyebrow-shaped stripes consistent with expression in floor cells; follicle cells at the posterior of the egg chamber also begin expressing *aos* at this time (Wasserman and Freeman, 1998). In *S. lebanonensis, aos* mRNA was not detectable at S9 (Fig. A3d), but by S10B and S11, mRNA was present in a dorsolateral band of cells posterior to the anterior cortex (Fig. A3e, 3g). Like *S. lebanonensis pnt* (Fig. 3d), the dorsolateral band of *aos* expression expanded more posteriorly in later stages (Fig. 3h, A3f), again likely overlapping with cells expressing *br*. This pattern is inconsistent with the midline "T" and floor-cell expression seen in *D. melanogaster*.

Capicua patterning confirms early EGF pathway discrepancies

The *pnt* and *aos* expression patterns represent a marked departure in *broad*-inhibiting elements of the EGF pathway between species; therefore, we asked how *br* might be activated in *S. lebanonensis* follicle cells by assessing the expression of the SOX protein Cic. In *D. melanogaster*, Cic is expressed uniformly in the follicle cell nuclei during early stages of oogenesis. At S10, Cic moves to the cytoplasm in dorsal anterior cells in response to Grk signaling; this redistribution ultimately de-represses *br* (Fig. 4a; Astigarraga et al. 2007). At S11, after Mirr has activated *br* expression in roof cells (Atkey et al. 2006; Fuchs et al. 2012), Cic moves back into the nucleus in a subset of dorsal anterior cells: in a thin stripe on the dorsal midline and in two small dorsolateral patches, partially overlapping with Mirr (Astigarra et al. 2007).

We hypothesized that a similar, perhaps slightly expanded domain of cytoplasmic Cic in *S. lebanonensis* would allow *br* expression in a dorsolateral band. To test this hypothesis, we used an antibody directed against the highly conserved C-terminal domain of Cic (Kim et al. 2011). Consistent with observations in *D. melanogaster*, Cic was expressed uniformly in all follicle cells in early oogenesis (Fig. 4b, e). At S10B, however, when the protein would normally clear from the nuclei in *D. melanogaster*, Cic was actually up-regulated in a 4-to-5-cell wide dorsolateral band that lies approximately 4 cells posterior from the anterior cortex (Fig. 4c). Cells anterior to the nuclei where Cic was highly expressed did down-regulate Cic, and cells posterior to the highly expressing cells also cleared Cic from the nucleus. The band of nuclear Cic was approximately 5–6 cell rows wide. Further to the posterior, cells expressed nuclear Cic at the baseline level observed in earlier stages of oogenesis. Later in oogenesis, the domain of nuclear Cic up-regulation expanded to 6–8 rows of cells (Fig. 4d). Thus, Cic expression differs dramatically from that in *D. melanogaster* and more closely resembles the pattern seen in later stages.

dpERK patterning demonstrates that the EGF pathway deviates upstream of Capicua

To test whether these differences in EGF pathway components are mediated by changes in gene regulation or by altered signaling, we investigated the response of follicle cells to the Grk morphogen by examining the pattern of activated MAP kinase (di-phosphorylated ERK, dpERK). In *D. melanogaster*, dpERK staining appears at S10A in a small patch of dorsal anterior follicle cells (Peri et al. 1999; Zartman et al. 2009). This midline "T" of expression first expands to include roof cells and then refines during S10B to two intensely staining, eyebrow- shaped stripes of cells that mark the floor cells (Fig. 5a), with less pronounced staining in a lateral and posterior ring that suggests "spectacles". By early S11, only floor cells exhibit dpERK staining. In *S. lebanonensis*, membrane-associated punctate staining in columnar cells at early S9 resolves into a diffuse cytoplasmic signal in a wide dorsal patch by late S9 or early S10A. At S10B, a single row of dorsal anterior follicle cells exhibit strong staining, but this signal becomes less intense as the pattern expands posteriorly in later stages (Fig. 5b–e). These observations demonstrate that the earliest steps in EGF patterning of dorsal-appendage cells differ in *S. lebanonensis.*

Dpp-pathway elements exhibit expected patterns

We next examined the possible contributions of the BMP pathway in distinguishing dorsal-appendage cell patterning between species. In *D. melanogaster*, the type I receptor, *thickveins* (*tkv)*, is expressed in two dorsolateral patches of cells at S10B (Fig. 6a; Mantrova et al. 1999; Yakoby et al. 2008). Based on the known dynamics of *tkv* expression and the role that the Dpp pathway plays in specifying anterior columnar cell fates (Peri and Roth 2000), we hypothesized that *S. lebanonensis tkv* would be expressed in several rows of cells spanning the dorsal midline at the anterior of the oocyte in S10 egg chambers. As predicted, *in situ* hybridization revealed *tkv* transcripts in approximately 4–5 rows of anterior follicle cells (Fig. 6b, c).

To evaluate a downstream readout of Dpp signaling, we analyzed the patterning of the activated (phosphorylated) form of Mothers against dpp, P-Mad. In *D. melanogaster* S10 egg chambers, P-Mad is found in 2–3 rows of anterior columnar follicle cells (Fig. 6d; Yakoby et al. 2008). At S10 in *S. lebanonensis*, P-Mad localization was similar but slightly expanded in 4–5 rows of anterior columnar follicle cells (Fig. 6e, h). At later stages in *D. melanogaster*, the P- Mad pattern remains high in several rows of ventral follicle cells but splits across the dorsal midline and overlaps with the anterior rows of Br-expressing cells (Fig. 6f; Yakoby et al. 2008). In *S. lebanonensis*, P-Mad localized in a pattern as anticipated from our observations of *br* expression. Instead of having the expression pattern split across the midline, P-Mad was maintained across the dorsal side of the egg chamber but in a slightly wider band of 7–8 rows of cells that tapered to a much slimmer ventral band (Fig. 6g, h).

Both *tkv* and P-Mad expression patterns in *S. lebanonensis* are consistent with what we know about Dpp's role in *D. melanogaster*. We therefore conclude that the Dpp pathway is most likely not a contributing factor in producing the observed differences in the DA-forming cell primordia in the two species.

S. lebanonensis grk gene structure is conserved but Grk protein sequence exhibits moderate differences

Some of the differences in EGF-pathway signaling between *S. lebanonensis* and *D. melanogaster* could be due to changes in the regulation of early patterning genes. For example, enhancers that respond to high levels of Grk and drive expression of *pnt* and *aos* on the dorsal midline could have lost binding sites for key regulatory factors, thereby eliminating midline expression of these genes in *D. melanogaster*. To explain the Capicua pattern in *S. lebanonensis*, the regulatory region would need to gain sites that drive expression in a dorsolateral band, or, post-transcriptional modifications that modulate the stability of the protein would have to change. These hypotheses are difficult to evaluate without a high-quality genome assembly and the ability to transform *S. lebanonensis* with constructs that test Cic distribution and function.

Another possibility is that the EGF receptor itself has changed, and these variations modify interactions with downstream components, producing an altered response. This explanation is less likely since both fly genomes encode only one EGF receptor, and in Drosophila, Egfr functions in multiple developmental contexts (reviewed by Lusk et al. 2017) and is therefore under considerable evolutionary constraint (Palsson et al. 2004). Indeed, BLAST predicts a 92% identity between the two species' intracellular domains and a 71% identity between the extracellular domains (data not shown).

A third explanation is that *D. melanogaster* and *S. lebanonensis* follicle cells have distinct downstream responses due to amino acid changes in Grk. Consistent with this hypothesis, the *S. lebanonensis* Grk ortholog exhibits 45% sequence similarity to the *D. melanogaster* Grk amino acid sequence across the entire protein and 54% similarity within the EGF domain (Fig. 7a). Nevertheless, these two proteins are more similar to each other than the three other Drosophila EGF ligands, Spitz, Keren, and Vein, are to Grk (Fig. 7a).

We sought to determine if amino acid changes in *D. melanogaster* and *S. lebanonensis* Grk are sufficient to cause distinct downstream responses in patterning the DA-forming primordia. EGF domain swaps between two of the EGFR-interacting ligands, Vein and Spitz, are sufficient to cause differential EGF pathway responses in some contexts (Schnepp et al. 1998). In other situations, however, ligand concentration, not the identity of the ligand itself, determines the developmental outcome (Austin et al. 2014). Previous studies using genomic regions to rescue grk^{null} mutants showed that expression of *Drosophila willistoni grk* in *D. melanogaster* can induce an ectopic dorsal ridge structure in eggshells (Niepielko and Yakoby 2014). Unfortunately, the available scaffold in *S. lebanonensis* (Vicoso and Bachtrog 2015) lacks potentially important upstream and downstream regulatory regions, and we were unable to bridge the gap with the flanking genes predicted by synteny, *D12* and *AKAP200*. Furthermore, genomic rescue constructs, although longer than the DNA available for *Scaptodrosophila*, express relatively poorly, and multiple copies are insufficient to completely rescue grk^{null} alleles (Neuman-Silberberg and Schüpbach 1994; Niepielko and Yakoby 2014). We therefore chose to use the *GAL4/UAS* system to test the activity of grk^{Sl}.

Sequence analyses of *S. lebanonensis* genomic DNA and a partial grk^{Sl} cDNA demonstrate that the gene structure and splice junctions are conserved between the two species (Fig. 7b).

Since we were unable to obtain the entire *grk*^{Sl} 3′-UTR via PCR, and proper regulation of *grk* transcript in *D. melanogaster* requires elements in both the 5′- and 3′-UTRs (Saunders and Cohen 1999; Thio et al. 2000), we relied on localization and translation signals in the *UASp* vector (Fig. 7c; Rørth 1998).

Grk^{Sl} is active in *D. melanogaster*

Changing *grk* dosage is sufficient to alter follicle cell patterning and resultant eggshells (Neuman-Silberberg and Schüpbach 1994). As such, we used a variety of temperatures to modulate expression of the germline-specific *MTD-GAL4* (Petrella et al. 2007) and drive expression of *grk*^{Sl}. We compared phenotypes of these eggs with those produced by flies expressing *grk*^{Dm} using the same *GAL4/UASp* system. We observed four types of eggshell morphology (Fig. 8a and Fig. A4). In addition to wild-type DAs, we found three classes of dorsalized eggshells: Class I eggs had fused DAs and/or ectopic DA material at the base; Class II eggs had an enlarged dorsal midline and laterally positioned DAs; and Class III eggs had DA material completely surrounding the anterior region. At all temperatures, eggs collected from *MTD>w*^{1118} females were overwhelmingly wild type. In contrast, eggs collected from *MTD>grk*^{Dm} females were either wild type or moderately dorsalized (Class I), with the percentage of defects increasing with increasing temperature. Similarly, eggs collected from *MTD>grk*^{Sl} females were dorsalized, but surprisingly, the penetrance and expressivity were higher than that observed for flies expressing *grk*^{Dm}; these phenotypes increased proportionally with increasing temperature. At 30°C, nearly all eggs expressing *grk*^{Sl} were severely dorsalized (Class III). Regardless of temperature, we did not observe eggshells with variable numbers of long, thin DAs.

The stronger phenotype produced by *grk*^{Sl} could be due to greater activity of the Grk^{Sl} protein, higher levels of *UASp-grk*^{Sl} expression, and/or differences in the localization or translational regulation of the *grk*^{Sl} and *grk*^{Dm} transcripts. In regard to these issues, the *UASp- grk*^{Dm} and *UASp-grk*^{Sl} constructs differ in two significant ways. The former was integrated into the genome at an unknown site by *P*-element transposition, whereas the latter was inserted at a known *attP* site; these properties could affect expression levels. Secondly, the *UASp-grk*^{Sl} construct lacks a portion of 3′-UTR, and this segment of DNA encodes elements important for mRNA localization (Saunders and Cohen 1999; Thio et al. 2000; Van de Boor 2005; Lan et al. 2010).

To examine mRNA localization and levels, we analyzed *grk*^{Sl} and *grk*^{Dm} transcripts by *in situ* hybridization. We found that the mRNA localization patterns of both *grk*^{Dm} and *grk*^{Sl} were consistent with the observed eggshell morphologies. Probes generated against each *grk* homolog do not cross-react between species (Fig. A5a, b). *grk*^{Dm} localization was wild-type in all stages of egg chambers dissected from control *MTD>w*^{1118} females (data not shown). In contrast, half of the egg chambers from females over-expressing *grk*^{Dm} at 30°C exhibited diffuse *grk*^{Dm} transcript at the anterior of the oocyte (Fig. A5c, d) rather than tightly localized to the anterodorsal corner, consistent with the percentage of laid eggs with moderate DA defects (Fig. 8a). In egg chambers expressing *Scaptodrosophila grk*, some *grk*^{Sl} transcript was localized correctly, but levels were high and excess transcript was present at the anterior end of the oocyte and highly abundant in the nurse cells, especially in

egg chambers at mid-to-late stages of oogenesis (Fig. A5e, f). Egg chambers from females placed at lower temperatures exhibited similar patterns but with commensurately lower numbers showing aberrant localization (data not shown). The grk^{Sl} mRNA localization in *D. melanogaster* was consistent with both the penetrance and expressivity of dorsalization phenotypes we observed across a range of temperatures (Fig. A4).

Grk^{Sl} expression in *D. melanogaster* alters follicle cell patterning

The morphological changes that we observed with our eggshell analyses were consistent with changes in patterning. We therefore examined the expression of Broad, the transcription factor that marks the roof cells of the DA primordia, in stage 10B egg chambers. We saw a range of Broad patterns that paralleled the severity of dorsalized eggshell phenotypes (Fig. 8b): wild-type Broad localization in two „patches'; Class I, two regions of Broad localization with a smaller midline, and in some cases, an absent midline; Class II, two regions of Broad localization with an enlarged midline; and Class III, a single, expanded primordium wrapped laterally around the anterior of the oocyte, with no midline present. The vast majority of control $MTD>w^{1118}$ egg chambers were wild type, while the most common phenotypes seen in $MTD>grk^{Dm}$ egg chambers altered the spacing of the midline; no egg chambers had an anterior „ring' of Broad localization. The majority of $MTD>grk^{Sl}$ egg chambers, on the other hand, did show an expanse of Broad encircling the oocyte. These data correlate with the distribution of eggshell phenotypes we observed and indicate that $MTD>grk^{Sl}$ eggshells are dorsalized because grk^{Sl} expression disrupts follicle cell patterning.

Grk^{Sl} expression in *D. melanogaster* does not mislocalize endogenous *grk* transcript or protein

Grk^{Sl} expression could alter Broad localization patterns in $MTD>grk^{Sl}$ eggshells by two potential means. First, it could be that the high levels of grk^{Sl} transcript compete away RNA-binding proteins required to properly localize the endogenous *grk* transcript and/or regulate its translation into protein. Modulating these regulatory factors could result in a broadened primordium. An alternate explanation is that the Grk^{Sl} protein is secreted and activates the overlaying follicle cells. To distinguish between these hypotheses, we used dual immunofluorescence and fluorescent *in situ* hybridization (IF/FISH) to examine both endogenous *D. melanogaster grk* transcript (Neuman-Silberberg and Schüpbach 1993) and protein (Neuman-Silberberg and Schüpbach 1996) in $MTD>grk^{Sl}$ egg chambers. The first hypothesis predicts a diffuse *grk*/Grk localization pattern (Fig. 9a, left), while the second hypothesis predicts a wild-type pattern of *grk*/Grk localization at the anterodorsal corner of the oocyte (Fig. 9a, right).

We categorized egg chambers based on aberrant localization of *grk* transcript and/or protein. Although most $MTD>w^{1118}$ egg chambers were wild type, a modest percentage of egg chambers had a diffuse Grk protein pattern (Fig. 9b; representative images 9c and d, respectively) consistent with the fraction of eggs laid at 30°C exhibiting DA defects. Because the IF/FISH method fluorescently labels all *D. melanogaster grk* transcript and protein, we observed, as expected, abundant levels of *grk* transcript in $MTD>grk^{Dm}$ egg chambers. Most $MTD>grk^{Dm}$ egg chambers deviated from wild type (Fig. 9b), but half of

these samples exhibited aberrant mRNA localization yet normal protein distribution (representative image 9e). Since only 50% of laid eggs exhibited DA defects (Fig. 8a), we speculate that egg chambers in which the transcript was mis-localized but the protein was wild type represent samples that would produce normal eggs; this phenotypic class was uniquely present in *MTD>grk^{Dm}* egg chambers. In *MTD>grk^{Sl}* egg chambers, most egg chambers exhibited wild-type levels and localization of *grk^{Dm}* mRNA and protein (Fig. 9b). In those cases where *grk* transcript was aberrant, Grk protein was also more dispersed. The percentage of *MTD>grk^{Sl}* egg chambers with a diffuse Grk localization pattern was somewhat higher relative to that seen in control *MTD>w^{1118}* egg chambers, but the majority of *MTD>grk^{Sl}* egg chambers still showed wild-type *grk*/Grk localization (Fig. 9b, c). These IF/FISH results contrast with the observation that 100% of laid eggs from *MTD>grk^{Sl}* females exhibited dorsalized eggshells. We conclude that the *S. lebanonensis* Grk homolog activates overlaying follicle cells in *D. melanogaster* mainly through its own activity and not by disrupting endogenous *grk.*

Discussion

EGF ligand-receptor interactions do not sufficiently explain patterning differences between species

In summary, our functional studies of *S. lebanonensis* Grk suggest that the protein elicits downstream EGF responses in *D. melanogaster* but does not produce changes in the tube-forming mechanism. The *UASp-grk^{Sl}* construct caused DA defects in a temperature-dependent manner, in accord with previous studies that perturbed *grk* gene dosage levels (Neuman-Silberberg and Schüpbach 1994).

The *grk^{Sl}* DA defects bear a close resemblance to those seen in *sqd* and *fs(1)K10* mutants (*squid*; Kelley 1993; *female sterile (1) K10*; Wieschaus et al. 1978). Sqd and K10 mediate transport of *grk* mRNA from the oocyte anterior cortex to the dorsal anterior corner, and they repress *grk* translation during this process (Kelley 1993; Neuman-Silberberg and Schüpbach 1993; Neuman-Silberberg and Schüpbach 1996; Norvell et al. 1999; Jaramillo et al. 2008; Cáceres and Nilson 2009). The similarity of phenotypes suggests that sequences critical for *grk* mRNA regulation are absent from the *UASp-grk^{Sl}* construct; alternatively, they do not share sufficient sequence or structural homology to mediate binding by Sqd and K10, leading to high levels of *grk^{Sl}* translation upon arrival at the oocyte. The *grk^{Sl}* transcript still localizes to the anterior, however, where it is unequivocally active, and *MTD>grk^{Sl}* egg chambers are severely dorsalized.

Changes in follicle cell fate (Br patterns) were due to high levels of Grk^{Sl} protein and not to mislocalized endogenous *grk* transcript and protein. As a comparison for ectopic expression of *grk^{Sl}*, we used a *UASp* construct to overexpress *grk^{Dm}*. Under the same temperature regimes, Grk^{Dm} produced a weaker response than Grk^{Sl}, likely due to differences in the structures and locations of the transgenes. At 25°C, *grk^{Sl}* expression in *MTD>grk^{Sl}* females was modest, and the mRNA localization pattern most closely resembled that found in *S. lebanonensis*. If the ligand were sufficient to alter the downstream response in follicle cells, one might expect multiple DAs under these conditions. These females, however, failed to produce eggs with multiple DAs; rather, eggshells exhibited a moderately dorsalized

phenotype compared to that seen at 30°C. More importantly, even at high, constitutive levels of grk^{Sl} expression, $MTD{>}grk^{Sl}$ females failed to produce any eggshells with multiple DAs.

These results suggest that although the Grk^{Sl} ligand is active, Grk^{Sl} expression is insufficient to alter the morphogenetic mechanism employed during DA formation. We therefore conclude that amino acid changes to Grk sequences are not sufficient to distinguish downstream responses between species. Our findings contrast with another study in which expression of *grk* from *D. willistoni* produced a dorsal ridge, an eggshell feature absent from *D. melanogaster* eggs (Niepielko and Yakoby 2014). Although *D. melanogaster* is more closely related to *D. willistoni* than it is to *S. lebanonensis*, the EGF domain protein sequences of *D. willistoni* and *S. lebanonensis* have the same level of homology (55%) with that of *D. melanogaster*, albeit not with each other. Our results suggest that early steps in the EGF signaling pathway, rather than changes to receptor-ligand interactions, distinguishes *D. melanogaster* and *S. lebanonensis* DA patterning.

Early EGF pathway components diverge and likely distinguish patterning between species

Based on our knowledge of DA-cell patterning in *D. melanogaster*, we examined EGF and BMP pathway components in *S. lebanonensis*. Although expression patterns alone do not demonstrate function, highly regulated transcript localization is a hallmark of *D. melanogaster* oogenesis and of animal development in general.

Given the domain of cells that create the DAs in *S. lebanonensis*, we observed the anticipated *tkv* and P-Mad expression patterns. These data are consistent with results from Niepielko and colleagues (2011), who examined P-Mad and *tkv* patterns in relation to Broad staining in 16 Drosophilid species. They found that all 16 species share early patterns of expression but resolve into four distinct classes at later stages (Niepielko et al. 2011). *S. lebabonensis* egg chambers exhibited these same early patterns of expression but produced a new pattern at S10B, a pattern appropriate for the single domain of DA-forming cells. The continued expansion of P-Mad into more posterior cells at S11/S12 was consistent with the proposed role for BMP signaling in shutting off *br* transcription at later stages (Yakoby et al. 2008). Our results suggest that the Dpp pathway is less likely to contribute to distinguishing DA patterning between the two species when compared to the EGF pathway.

In contrast, although *grk* transcript localization in *S. lebanonensis* did not differ significantly from *D. melanogaster*, early responses to EGF activation, including dpERK, revealed distinct and dynamic expression patterns. At S10B, when expression began to reveal EGF activity associated with DV patterning, the downstream components, *pnt*, *aos*, and Cic exhibited distributions that more closely resembled expression patterns occurring at later stages (S12) in *D. melanogaster*. At S10B in *D. melanogaster*, columnar follicle cells express either *pnt*, *br*, or nuclear Cic, but in *S. lebanonensis*, follicle cells expressed various combinations of *pnt* alone, *br* alone, *br* and nuclear Cic together, or all three transcription factors (Fig. 10). It will be important to confirm the co-expression of *pnt* and *br* at the protein level in conjunction with the observed nuclear Cic patterning.

How is *br* activated in the presence of nuclear Cic and Pnt, two of its upstream inhibitors? One likely explanation lies in alterations to cis-regulatory regions, which are well- known

drivers of evolutionary change (Carroll 2008). To date, there are two characterized *br* enhancer regions that are required for DA formation in *D. melanogaster* (Cheung et al. 2013; Revaitis et al. 2017). Changes in these enhancers, or the presence of additional enhancers unresponsive to Pnt and Cic, could ensure robust levels of *br*.

With regards to the *pnt* and *aos* expression patterns, a loss of binding sites for regulatory factors that respond to high levels of Grk could accommodate expression in dorsolateral cells without induction on the midline. Since *pnt*, *aos*, and Cic expression in *S. lebanonensis* resemble patterns seen in later stages in *D. melanogaster*, stages associated with tube elongation, this heterochronic shift to a „later stage' pattern could provide clues as to why *S. lebanonensis* tubulogenesis occurs without wrapping.

Questions remain about embryonic DV patterning

The Cic pattern raises important questions about the relationship between DA patterning during oogenesis and embryonic DV patterning. In *D. melanogaster*, the de-repression of *mirr* in response to EGF activation (via exclusion of Cic from nuclei) inhibits *pipe* expression in dorsal follicle cells (Goff et al. 2001). *pipe* encodes a sulfotransferase that normally modifies proteins in the innermost layer of the ventral eggshell; this regional alteration initiates a serine-protease cascade during embryogenesis that ultimately activates Dorsal, which establishes DV polarity (reviewed by Stein and Stevens 2014). Thus, nuclear Cic in *S. lebanonensis* could allow *pipe* expression in dorsal follicle cells, disrupting embryonic polarity. We hypothesize that changes have occurred to a *mirr* enhancer that would disjoin DA patterning from embryonic patterning.

Vreede et al. (2013) examined this relationship by looking at patterning in a species that lacks DAs, *Ceratitis capitata*. Their study showed that *pipe* is still expressed in a ventral pattern, suggesting that the EGF-derived positional information that establishes embryonic polarity predates EGF patterning of the DA primordium. The authors propose that *mirr* is a key evolutionary node and put forth a model in which multiple *mirr* enhancers respond to different inputs: a putative ancestral enhancer, *mirLo*, would respond to intermediate levels of EGF to establish DV polarity, while an acquired enhancer in *D. melanogaster*, *mirHi*, would integrate both Dpp and high EGF signals to specify follicle cells for DA formation. Presumably, the *mirLo* enhancer region would be present in *S. lebanonensis*, but the *mirHi* enhancer is modified such that a DA primordium still forms without disrupting embryonic polarity.

DA morphology and patterning in the last common ancestor between *D. melanogaster* and *S. lebanonensis* are unknown. Therefore, key enhancer regions could have been 'lost' in *S. lebanonensis*, or they are derived features of *D. melanogaster* patterning. We hypothesize that the downstream consequences will contribute to different mechanisms of morphogenesis.

Are differences in development timing environmental adaptations between species?

Our work with a non-model Drosophilid species has given rise to many unanswered questions regarding environmental adaptations and DA morphology. We and others have posited that DA number and morphology are intricately linked to egg-laying behavior and

environment (Kambysellis and Heed 1971; James and Berg 2003; Kagesawa et al. 2008). As DAs supply oxygen to the developing embryo, it is tempting to postulate that *S. lebanonensis* has evolved an eggshell morphology suited for optimizing embryo development at lower oxygen levels, as females tend to bury their eggs deep into the food. Additional studies are needed to determine the mechanisms that regulate the number of DAs produced by each egg chamber.

S. lebanonensis ovarioles develop synchronously within a single female and with different timing compared to *D. melanogaster*. This synchrony is similar to developmental processes in some other Drosophilid species, including *D. aldrichi, D. mulleri, D. repleta*, and *Scaptodrosophila victoria* (Kambysellis 1968). Intra-clutch synchrony exists elsewhere in the animal kingdom, for example in sea turtles, snakes, and birds (Santos et al. 2016; Aubret et al. 2016; Webster et al. 2015), but is generally considered an anti-predator strategy. Rather than preventing predation, it is possible that synchrony in *S. lebanonensis* facilitates survival of post- embryonic stages on ephemeral food resources or allows the female to lay a clutch of eggs and thereby minimize her effort during oviposition (Kambysellis and Heed 1971). In *S. lebanonensis*, hormonal cues might regulate germline stem cell divisions in response to sufficient levels of nutrients.

Conclusions

We find that the EGF pathway diverges at the earliest steps between *D. melanogaster* and *S. lebanonensis*, particularly in the expression of dpERK, *pnt, aos*, and nuclear Cic. The *S. lebanonensis grk* expression pattern does not explain the pattern of these early EGF components, nor does the Grk^{Sl} protein. Nonetheless, the EGF response downstream of *grk* yields a single *br* primordium from which a variable number of dorsal appendages can arise. Beyond EGF patterning and DA morphology, Osterfield and colleagues have shown that cell shape changes and migration in *Scaptodrosophila* vary dramatically from what is known in *D. melanogaster* (Osterfield et al. 2013). To gain further insight into what initiates and regulates different cellular behaviors to create a homologous structure, it will be necessary to identify the downstream genes that are regulated by this novel combination of patterning genes.

Supplementary Material

Refer to Web version on PubMed Central for supplementary material.

Acknowledgments

We thank Sydney Bowker, Vincent So, and Jill Kumasaka for help with *in situ* hybridization experiments, Dr. Scott Roy at San Francisco State University for advice on *Scaptodrosophila* gene annotation, Dr. Robert Waterston and Dr. Evan Eichler for the use of their compound microscopes, and Dr. Miriam Osterfield and members of the Berg lab for helpful discussions. For technical support and advice on imaging, we thank Dr. Nathaniel Peters at the University of Washington W. M. Keck Imaging Center, which is supported by the National Institutes of Health (NIH) grant 1S10 OD016240. We are grateful to FlyBase for exceptional genetic, genomic, and bibliographic resources, the Bloomington Drosophila Stock Center for the *MTD-GAL4* driver, the Drosophila Genomics Resource Center for the *UASp-attB* plasmid, the Drosophila Species Stock Center (formerly at Bowling Green and Tucson but now in San Diego) for providing *Scaptodrosophila lebanonensis* flies, and Drs. Norbert Perrimon and Christian Ghiglione for the *UASp-grk.mb* strain. We thank Dr. Tom Jessell and colleagues E. Laufer, S. Morton, and D. Vasiliauskas for antibody against phosphorylated Smad1/5/8 (P-Mad). We obtained anti- Gurken, anti-

Broad, and anti-DE-Cadherin monoclonal antibodies from the Developmental Studies Hybridoma Bank, created by the National Institute of Child Health and Human Development of the National Institutes of Health and maintained by the University of Iowa, Department of Biology. Funding from the National Institutes of Health grant R01-GM079433 (C.A.B.) supported this work.

References

Astigarraga S, Grossman R, Díaz-Delfín J, Caelles C, Paroush Z, Jiménez G. A MAPK docking site is critical for downregulation of Capicua by Torso and EGFR RTK signaling. EMBO J. 2007; 26:668–677. [PubMed: 17255944]

Atkey MR, Boisclair Lachance JB, Walczak M, Rebello T, Nilson LA. Capicua regulates follicle cell fate in the *Drosophila* ovary through repression of *mirror*. Development. 2006; 133:2115–2123. [PubMed: 16672346]

Aubret F, Blanvillain G, Bignon F, Kok PJR. Heartbeat, embryo communication and hatching synchrony in snake eggs. Sci Rep. 2016; 6:23519. [PubMed: 26988725]

Austin CL, Manivannan SN, Simcox A. TGF-α ligands can substitute for the neuregulin Vein in *Drosophila* development. Development. 2014; 141:4110–4114. [PubMed: 25336739]

Bächli G, Haring E, Vilela CR. On the phylogenetic relationships of *Scaptodrosophila rufifrons S. lebanonensis* (Diptera, Drosophilidae). Journal of the Swiss Entomological Society. 2005; 78:349–36.

Berg CA. The *Drosophila* shell game: patterning genes and morphological change. Trends Genet. 2005; 21:346–355. [PubMed: 15922834]

Boisclair Lachance JB, Lomas MF, Eleiche A, Kerr PB, Nilson LA. Graded Egfr activity patterns the *Drosophila* eggshell independently of autocrine feedback. Development. 2009; 136:2893–2902. [PubMed: 19641015]

Cáceres L, Nilson LA. Translational repression of *gurken* mRNA in the Drosophila oocyte requires the hnRNP Squid in the nurse cells. Dev Biol. 2009; 326:327–334. [PubMed: 19100729]

Carroll SB. Evo-devo and an expanding evolutionary synthesis: a genetic theory of morphological evolution. Cell. 2008; 134:25–36. [PubMed: 18614008]

Cheung LS, Simakov DSA, Fuchs A, Pyrowolakis G, Shvartsman SY. Dynamic model for the coordination of two enhancers of *broad* by EGFR signaling. Proc Natl Acad Sci USA. 2013; 110:17939–17944. [PubMed: 24127599]

Deng WM, Bownes M. Two signalling pathways specify localised expression of the *Broad-Complex* in *Drosophila* eggshell patterning and morphogenesis. Development. 1997; 124:4639–4647. [PubMed: 9409680]

DiBello PR, Withers DA, Bayer CA, Fristrom JW, Guild GM. The *Drosophila Broad-Complex* encodes a family of related proteins containing zinc fingers. Genetics. 1991; 129:385–397. [PubMed: 1743483]

Dobens LL, Peterson JS, Treisman J, Raftery LA. *Drosophila bunched* integrates opposing DPP and EGF signals to set the operculum boundary. Development. 2000; 127:745–754. [PubMed: 10648233]

Dorman JB, James KE, Fraser SE, Kiehart DP, Berg CA. *bullwinkle* is required for epithelial morphogenesis during *Drosophila* oogenesis. Dev Biol. 2004; 267:320–341. [PubMed: 15013797]

Fuchs A, Cheung LS, Charbonnier E, Shvartsman SY, Pyrowolakis G. Transcriptional interpretation of the EGF receptor signaling gradient. Proc Natl Acad Sci USA. 2012; 109:1572–1577. [PubMed: 22307613]

Ghiglione C, Bach EA, Paraiso Y, Carraway KL, Noselli S, Perrimon N. Mechanism of activation of the *Drosophila* EGF receptor by the TGFα ligand Gurken during oogenesis. Development. 2002; 129:175–186. [PubMed: 11782411]

Goentoro LA, Reeves GT, Kowal CP, Martinelli L, Schüpbach T, Shvartsman SY. Quantifying the Gurken morphogen gradient in *Drosophila* oogenesis. Dev Cell. 2006; 11:263–272. [PubMed: 16890165]

Goff DJ, Nilson LA, Morisato D. Establishment of dorsal-ventral polarity of the *Drosophila* egg requires *capicua* action in ovarian follicle cells. Development. 2001; 128:4553–4562. [PubMed: 11714680]

Golembo M, Schweitzer R, Freeman M, Shilo BZ. *argos* transcription is induced by the *Drosophila* EGF receptor pathway to form an inhibitory feedback loop. Development. 1996; 122:223–230. [PubMed: 8565833]

Hinton HE. The structure and function of the respiratory horns of the eggs of some flies. Philos Trans R Soc Lond B. 1960; 243:45–73.

Horne-Badovinac S, Bilder D. Mass transit: epithelial morphogenesis in the *Drosophila* egg chamber. Dev Dyn. 2005; 232:559–574. [PubMed: 15704134]

Hudson AM, Cooley L. Methods for studying oogenesis. Methods. 2014; 68:207–217. [PubMed: 24440745]

Jaramillo AM, Weil TM, Goodhouse J, Gavis ER, Schüpbach T. The dynamics of fluorescently labeled endogenous *gurken* mRNA in Drosophila. J Cell Sci. 2008; 121:887–894. [PubMed: 18303053]

James KE, Berg CA. Temporal comparison of Broad-Complex expression during eggshell-appendage patterning and morphogenesis in two *Drosophila* species with different eggshell-appendage numbers. Gene Expr Patterns. 2003; 3:629–634. [PubMed: 12971997]

Kagesawa T, Nakamura Y, Nishikawa M. Distinct activation patterns of EGF receptor signaling in the homoplastic evolution of eggshell morphology in genus *Drosophila*. Mech Dev. 2008; 125:1020–1032. [PubMed: 18762251]

Kambysellis MP, Heed WB. Studies of oogenesis in natural populations of Drosophilidae. I. Relation of ovarian development and ecological habitats of the Hawaiian species. Am Nat. 1971; 105:31–49.

Kambysellis, MP. Comparative studies of oogenesis and egg morphology among species of the genus *Drosophila*. In: Wheeler, MR., editor. Studies in Genetics IV. Research Reports Univ Tex Publ 6818; Austin TX: 1968. p. 71-92.

Kelley RL. Initial organization of the Drosophila dorsoventral axis depends on an RNA- binding protein encoded by the *squid* gene. Genes Dev. 1993; 7:948–960. [PubMed: 7684991]

Kim Y, Andreu MJ, Lim B, Chung K, Terayama M, Jiménez G, Berg CA, Lu H, Shvartsman SY. Gene regulation by MAPK substrate competition. Dev Cell. 2011; 20:880–887. [PubMed: 21664584]

King, RC. Drosophila melanogaster. Academic Press; New York: 1970. Ovarian development.

Klämbt C. The *Drosophila* gene *pointed* encodes two ETS-like proteins which are involved in the development of the midline glial cells. Development. 1993; 117:163–176. [PubMed: 8223245]

Klein DE, Nappi VM, Reeves GT, Shvartsman SY, Lemmon MA. Argos inhibits epidermal growth factor receptor signalling by ligand sequestration. Nature. 2004; 117:163–176.

Lan L, Lin S, Zhang S, Cohen RS. Evidence for a transport-trap mode of *Drosophila melanogaster gurken* mRNA localization. PLoS ONE. 2010; 5:e1544.

Lembong J, Yakoby N, Shvartsman SY. Spatial regulation of BMP signaling by patterned receptor expression. Tissue Eng Part A. 2008; 14:1469–1477. [PubMed: 18707227]

Lin H, Spradling AC. Germline stem cell division and egg chamber development in transplanted *Drosophila* germaria. Dev Biol. 1993; 159:140–152. [PubMed: 8365558]

Lobell AS, Kaspari RR, Negron YLS, Harbison ST. The genetic architecture of ovariole number in *Drosophila melanogaster*: genes with major, quantitative, and pleiotropic effects. G3. 2017; 7:2391–2403. [PubMed: 28550012]

Lubarsky B, Krasnow MA. Tube morphogenesis: making and shaping biological tubes. Cell. 2003; 112:19–28. [PubMed: 12526790]

Lusk JB, Lam VYM, Tolwinski NS. Epidermal growth factor pathway signaling in *Drosophila* embryogenesis: tools for understanding cancer. Cancers. 2017; 9:E16. [PubMed: 28178204]

Mantrova EY, Schulz RA, Hsu T. Oogenic function of the myogenic factor D-MEF2: negative regulation of the Decapentaplegic receptor gene *thick veins*. Proc Natl Acad Sci USA. 1999; 96:11889–11894. [PubMed: 10518546]

Morimoto AM, Jordan KC, Tietze K, Britton JS, O'Neill EM, Ruohola-Baker H. Pointed, an ETS domain transcription factor, negatively regulates the EGF receptor pathway in *Drosophila* oogenesis. Development. 1996; 122:3745–3754. [PubMed: 9012496]

Neuman-Silberberg FS, Schüpbach T. The *Drosophila* dorsoventral patterning gene *gurken* produces a dorsally localized RNA and encodes a TGF α-like protein. Cell. 1993; 75:165–174. [PubMed: 7691414]

Neuman-Silberberg FS, Schüpbach T. Dorsoventral axis formation in *Drosophila* depends on the correct dosage of the gene *gurken*. Development. 1994; 120:2457–2463. [PubMed: 7956825]

Neuman-Silberberg FS, Schüpbach T. The *Drosophila* TGF-α-like protein Gurken: expression and cellular localization during *Drosophila* oogenesis. Mech Dev. 1996; 59:105–113. [PubMed: 8951789]

Niepielko MG, Hernáiz-Hernández Y, Yakoby N. BMP signaling dynamics in the follicle cells of multiple *Drosophila* species. Dev Biol. 2011; 354:151–159. [PubMed: 21402065]

Niepielko MG, Yakoby N. Evolutionary changes in TGFα distribution underlie morphological diversity in eggshells from *Drosophila* species. Development. 2014; 141:4710–4715. [PubMed: 25468939]

Norvell A, Kelley RL, Wehr K, Schüpbach T. Specific Isoforms of Squid, a Drosophila hnRNP, perform distinct roles in *gurken* localization during oogenesis. Genes Dev. 1999; 13:864–876. [PubMed: 10197986]

O'Neill EM, Rebay I, Tjian R, Rubin GM. The activities of two Ets-related transcription factors required for *Drosophila* eye development are modulated by the Ras/MAPK pathway. Cell. 1994; 78:137–147. [PubMed: 8033205]

Osterfield M, Berg CA, Shvartsman SY. Epithelial patterning, morphogenesis, and evolution: *Drosophila* eggshell as a model. Dev Cell. 2017; 41:337–348. [PubMed: 28535370]

Osterfield M, Schüpbach T, Wieschaus E, Shvartsman SY. Diversity of epithelial morphogenesis during eggshell formation in drosophilids. Development. 2015; 142:1971–1977. [PubMed: 25953345]

Palsson A, Rouse A, Riley-Berger R, Dworkin I, Gibson G. Nucleotide Variation in the *Egfr* Locus of *Drosophila melanogaster*. Genetics. 2004; 167:1199–1212. [PubMed: 15280235]

Peri F, Bökel C, Roth S. Local Gurken signaling and dynamic MAPK activation during Drosophila oogenesis. Mech Dev. 1999; 81:75–88. [PubMed: 10330486]

Peri F, Roth S. Combined activities of Gurken and Decapentaplegic specify dorsal chorion structures of the *Drosophila* egg. Development. 2000; 127:841–850. [PubMed: 10648242]

Petrella LN, Smith-Leiker T, Cooley L. The Ovhts polyprotein is cleaved to produce fusome and ring canal proteins required for *Drosophila* oogenesis. Development. 2007; 134:703–712. [PubMed: 17215303]

Pyrowolakis G, Veikkolainen V, Yakoby N, Shvartsman SY. Gene regulation during *Drosophila* eggshell patterning. Proc Natl Acad Sci USA. 2017; 114:5808–5813. [PubMed: 28584108]

Revaitis NT, Marmion RA, Farhat M, Ekiz V, Wang W, Yakoby N. Simple expression domains are regulated by discrete CRMs during *Drosophila* oogenesis. G3. 2017; 7:2705–2718. [PubMed: 28634244]

Rørth P. Gal4 in the *Drosophila* female germline. Mech Dev. 1998; 78:113–118. [PubMed: 9858703]

Santos RG, Pinheiro HT, Martins AS, Riul P, Bruno SC, Janzen FJ, Ioannou CC. The anti-predator role of within-nest emergence synchrony in sea turtle hatchlings. Proc R Soc Lond B. 2016; 283:20160697.

Saunders C, Cohen RS. The role of oocyte transcription, the 5′UTR, and translation repression and derepression in *Drosophila gurken* mRNA and protein localization. Mol Cell. 1999; 3:43–54. [PubMed: 10024878]

Schneider CA, Rasband WS, Eliceiri KW. NIH Image to ImageJ: 25 years of image analysis. Nat Methods. 2012; 9:671–675. [PubMed: 22930834]

Schnepp B, Donaldson T, Grumbling G, Ostrowski S, Schweitzer R, Shilo BZ, Simcox A. EGF domain swap converts a *Drosophila* EGF receptor activator into an inhibitor. Genes Dev. 1998; 12:908–913. [PubMed: 9531530]

Schüpbach T. Germ line and soma cooperate during oogenesis to establish the dorsoventral pattern of egg shell and embryo in *Drosophila melanogaster*. Cell. 1987; 49:699–707. [PubMed: 3107840]

Spradling, AC. Developmental genetics of oogenesis. In: Bate, M., Martinez-Arias, A., editors. The Development of Drosophila melanogaster, Vol 1. Cold Spring Harbor Press; New York: 1993. p. 1-70.

Stein DS, Stevens LM. Maternal control of the *Drosophila* dorsal-ventral body axis. Wiley Interdiscip Rev Dev Biol. 2014; 3:301–330. [PubMed: 25124754]

Thio GL, Ray RP, Barcelo G, Schüpbach T. Localization of *gurken* RNA in *Drosophila* oogenesis requires elements in the 5′ and 3′ regions of the transcript. Dev Biol. 2000; 221:435–446. [PubMed: 10790337]

Twombly V, Blackman RK, Jin H, Graff JM, Padgett RW, Gelbart WM. The TGF-β signaling pathway is essential for *Drosophila* oogenesis. Development. 1996; 122:1555–1565. [PubMed: 8625842]

Tzolovsky G, Deng WM, Schlitt T, Bownes M. The function of the *Broad-Complex* during *Drosophila melanogaster* oogenesis. Genetics. 1999; 153:1371–1383. [PubMed: 10545465]

Van De Bor V, Hartswood E, Jones C, Finnegan D, Davis I. *gurken* and the *I* factor retrotransposon RNAs share common localization signals and machinery. Dev Cell. 2005; 9:51–62. [PubMed: 15992540]

Van der Meer JM. Optical clean and permanent whole mount preparation for phase- contrast microscopy of cuticular structures of insect larvae. Dros Inf Serv. 1977; 52:160.

Vicoso B, Bachtrog D. Numerous transitions of sex chromosomes in Diptera. PLoS Biol. 2015; 13:e1002078. [PubMed: 25879221]

Vreede BM, Lynch JA, Roth S, Sucena E. Co-option of a coordinate system defined by the EGFr and Dpp pathways in the evolution of a morphological novelty. Evo Devo. 2013; 4:7.

Wasserman JD, Freeman M. An autoregulatory cascade of EGF receptor signaling patterns the *Drosophila* egg. Cell. 1998; 95:355–364. [PubMed: 9814706]

Webster B, Hayes W, Pike TW. Avian egg odour encodes information on embryo sex, fertility and development. PLoS ONE. 2015; 10:e011634.

Wieschaus E, Marsh JL, Gehring W. *fs(1)K10*, a germline-dependent female sterile mutation causing abnormal chorion morphology in *Drosophila melanogaster*. Wilh Roux's Arch Dev Biol. 1978; 184:75–82.

Yakoby N, Lembong J, Schüpbach T, Shvartsman SY. *Drosophila* eggshell is patterned by sequential action of feedforward and feedback loops. Development. 2008; 135:343–351. [PubMed: 18077592]

Zartman JJ, Kanodia JS, Cheung LS, Shvartsman SY. Feedback control of the EGFR signaling gradient: superposition of domain-splitting events in Drosophila oogenesis. Development. 2009; 136:2903–2911. [PubMed: 19641013]

Zimmerman SG, Peters NC, Altaras AE, Berg CA. Optimized RNA ISH, RNA FISH and protein-RNA double labeling (IF/FISH) in *Drosophila* ovaries. Nat Protoc. 2013; 8:2158–2179. [PubMed: 24113787]

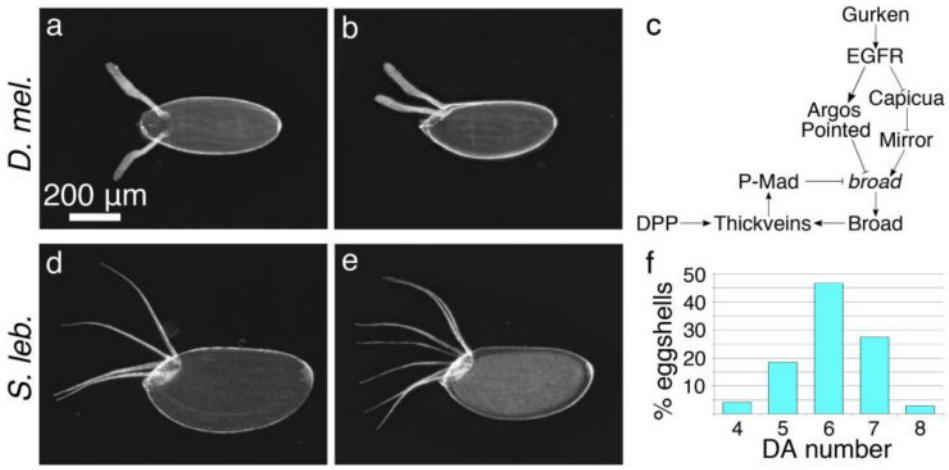

Fig. 1. *Scaptodrosophila* dorsal appendages are distinct from those of *D. melanogaster*

(a, b) *D. melanogaster* eggshells have two oar-shaped DAs with long stalks and flat paddles. Dorsal and lateral views are shown, respectively. (c) Two pathways define the DA primordia by controlling expression of *broad*. EGF signaling regulates *broad* expression as a function of ligand (*gurken)* concentration (see text). DPP signaling acts in a negative feedback loop with Broad. (d, e, f) *S. lebanonensis* eggs have 4–8 long, thin DAs. (d, e) Lateral views of eggs with 4 DAs and 7 DAs, respectively. (f) Distribution of DA number; N = 539.

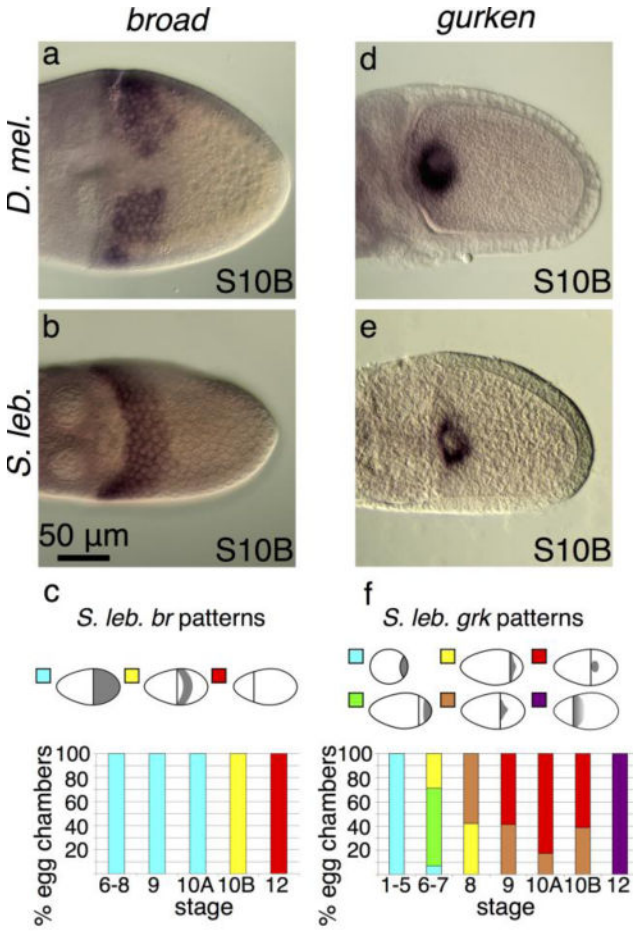

Fig. 2. A single *broad* DA primordium is not the result of different *gurken* expression patterns

All egg chambers are shown in a dorsal orientation unless otherwise noted. (a) *D. melanogaster br* is expressed in two dorsolateral patches. (b) *S. lebanonensis br* is expressed in a 6-cell band of follicle cells that spans the dorsal midline. (c) Quantitation of *S. lebanonensis br* expression; N > 10 for each stage category. (d) *D. melanogaster grk* is tightly localized around the oocyte nucleus. (e) *S. lebanonensis grk* is also tightly localized around the oocyte nucleus. (f) Quantitation of *S. lebanonensis grk* expression; N > 10 for each stage category.

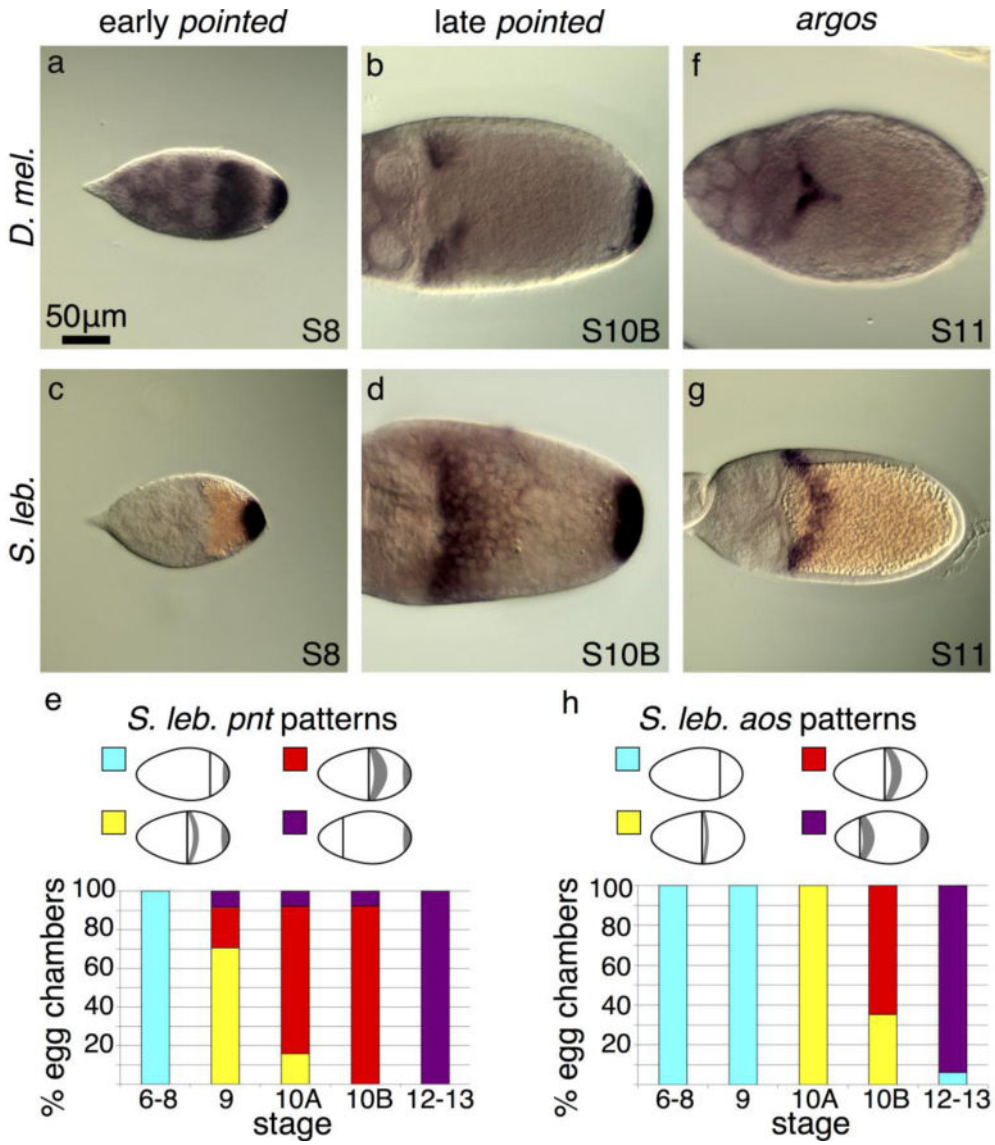

Fig. 3. *broad*-inhibiting elements are expressed in unexpected regions

(a) A probe designed to a common region of both *pnt* transcripts, *P1* and *P2*, reveals their combined expression patterns at S8 in *D. melanogaster*. P1 is expressed in posterior follicle cells and P2 is expressed at the anterior of the oocyte (Morimoto et al. 1996). At S10 (not shown), the P2 expression pattern refines into a T shape across the dorsal midline (similar to the *D. melanogaster aos* image shown in f). (b) In late *D. melanogaster* stages, the common-region probe reveals *pnt* P1 expression persisting in the posterior follicle cells while *P1* and *P2* expression in the anterior splits into two dorsolateral patches of follicle cells. (c) In *S. lebanonensis*, a probe to the predicted common region shows that early-stage egg chambers express *pnt* only in the posterior follicle cells. (d) In late stages, *S. lebanonensis pnt* is maintained in posterior follicle cells and now also appears in a dorsolateral band of 4–5 rows of anterior follicle cells. (e) Quantitation of *S. lebanonensis pnt* patterning; N > 10 for each stage category. (f) *D. melanogaster aos* expression is limited to a small peak above the oocyte nucleus starting at S11. (g) *S. lebanonensis aos* is expressed in a dorsolateral band of

follicle cells. (h) Quantitation of *S. lebanonensis aos* patterning; N > 10 for each stage category.

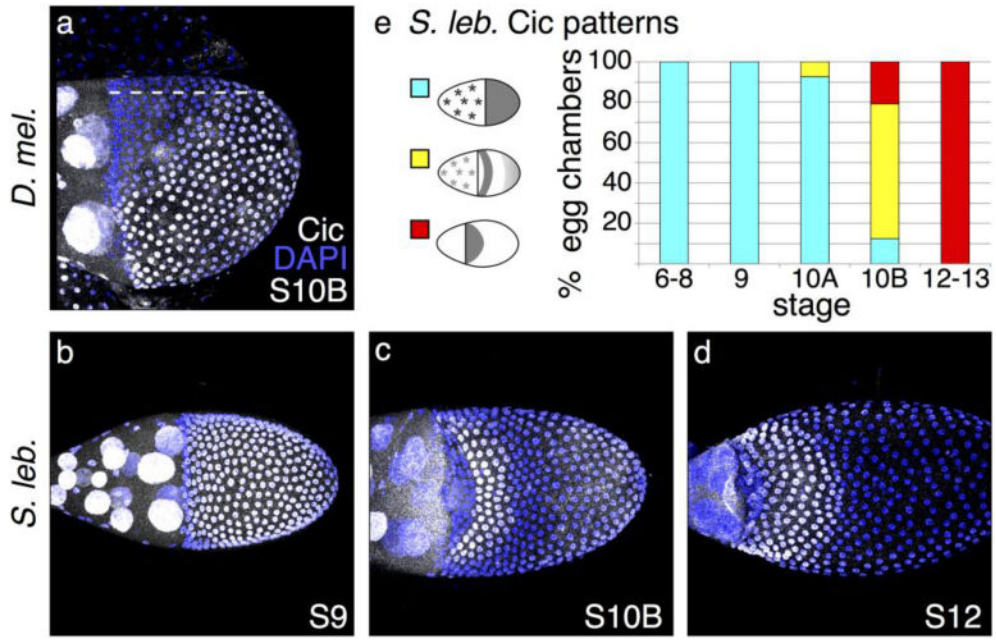

Fig. 4. Cic patterning confirms early EGF pathway discrepancies

(a) Lateral view of *D. melanogaster* egg chamber; dotted line marks the dorsal midline. At S10B, Cic is in the nucleus of most follicle cells but clears from the nuclei of cells that lie above the dorsal anterior corner of the oocyte. (b) In early stages of *S. lebanonensis* oogenesis, Cic is present in all follicle cell nuclei, similar to early *D. melanogaster* Cic localization. (c) By S10B in *S. lebanonensis*, Cic is present in nuclei in a band of 4–5 rows of cells across the dorsal midline, 4 rows to the posterior of the anterior cortex. Nuclei of posterior follicle cells exhibit weak staining. (d) At S12, Cic remains present in the nuclei of anterior cells and has expanded to 7–8 rows. (e) Quantitation of *S. lebanonensis* Cic localization; N > 10 for each stage category.

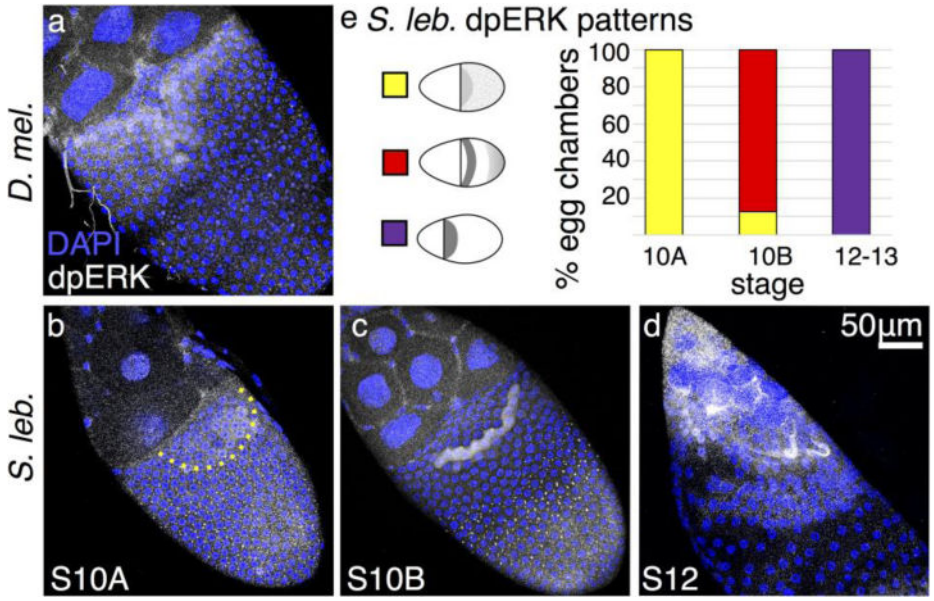

Fig. 5. dpERK patterning reveals early EGF-pathway discrepancies upstream of Cic

(a–d) Anterior is to the upper left, dorsal is facing out of the page. (a) At S10B in *D. melanogaster*, dpERK is present most strongly in floor cells, with weaker localization in roof cells. (b) In *S. lebanonensis*, dpERK is present at S10A in a punctate pattern in most columnar follicle cells, but a rounded patch of dorsal anterior cells exhibit diffuse cytoplasmic staining; boundary marked by dashed line. (c) At S10B, the punctate dpERK pattern is restricted to the posterior follicle cells. Intense cytoplasmic dpERK staining appears in one band of follicle cells located 4– 5 rows to the posterior of the anterior cortex. (d) At S12, dpERK remains diffuse in anterior cells and has expanded to additional rows more posteriorly. (e) Quantitation of *S. lebanonensis* dpERK localization; N > 15 for each stage except for S12, where N=7.

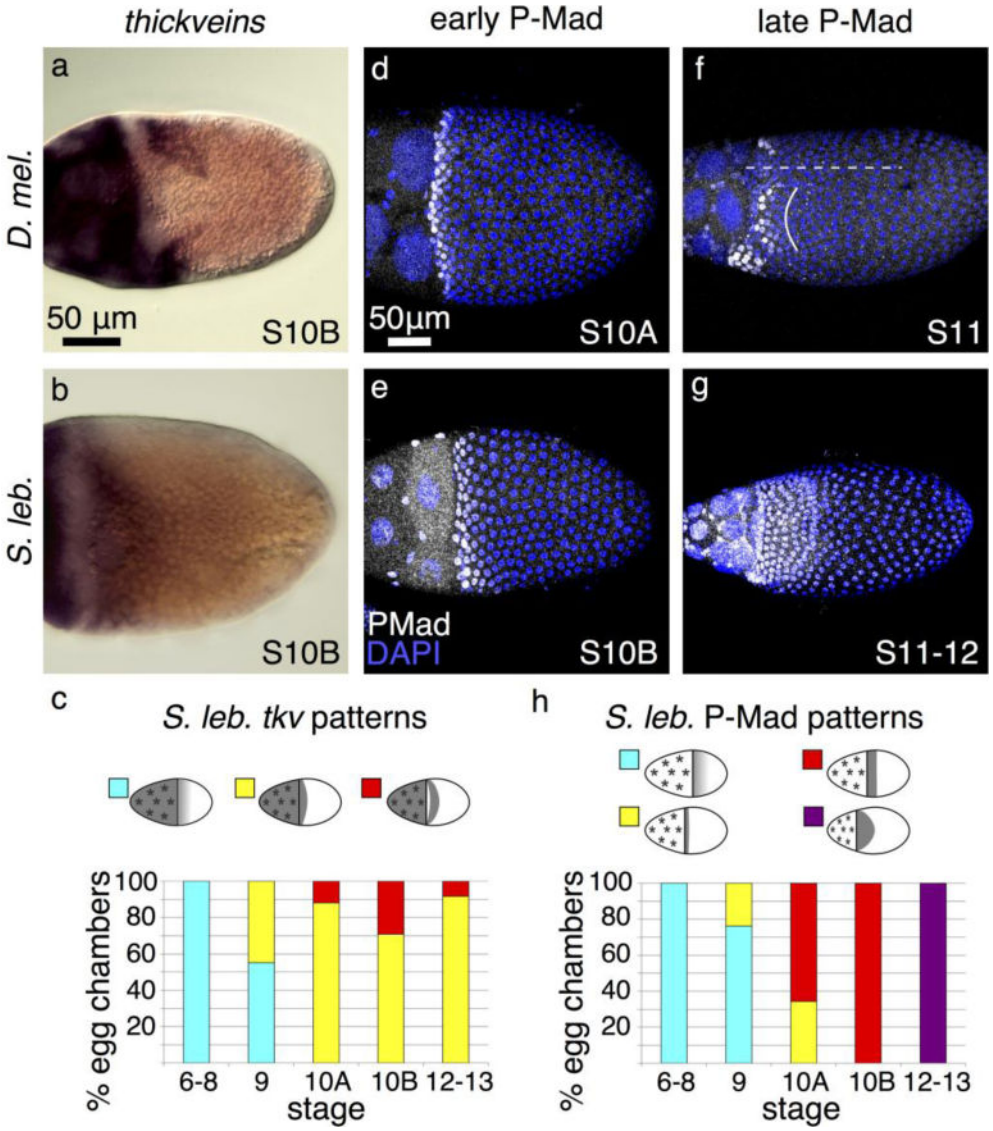

Fig. 6. Dpp-pathway elements exhibit expected patterns

(a) *D. melanogaster tkv* is expressed in nurse cells, stretch cells, and two dorsolateral patches of columnar follicle cells. (b) *S. lebanonensis tkv* is expressed in nurse cells, stretch cells, and 4–5 rows of dorso-anterior columnar follicle cells. (c) Quantitation of *S. lebanonensis tkv* expression; N > 10 for each stage category. (d) At S10A in *D. melanogaster*, P-Mad is present in a 2–3-row ring of follicle cells at the anterior of the oocyte. (e) At a slightly later stage in *S. lebanonensis*, P-Mad is present in a 4–5-row-wide ring of anterior follicle cells. Some cells have begun to migrate centripetally and are no longer visible in this plane. (f) This dorsolateral view of a S11 *D. melanogaster* egg chamber shows that P-Mad is restricted to two symmetrical patches (left patch marked by a solid curved line) on each side of the dorsal midline (dashed line). (g) By late S11/early S12 in *S. lebanonensis*, P-Mad expands posteriorly to 7 rows of follicle cells. (h) Quantitation of *S. lebanonensis* P-Mad localization; N > 10 for each stage category.

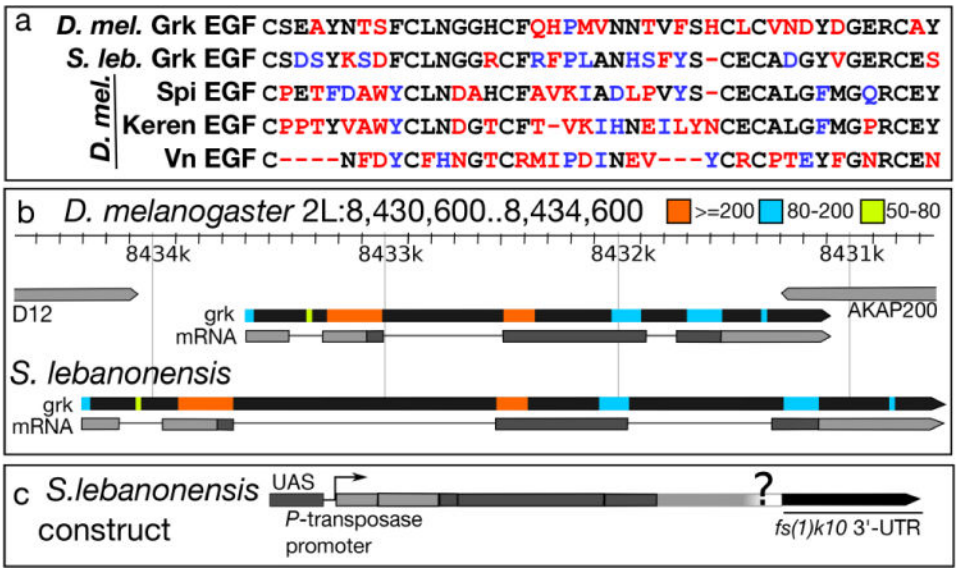

Fig. 7. Comparisons of *S. lebanonensis* and *D. melanogaster* Grk protein and gene sequences reveal significant homology

(a) Amino acid alignment of the EGF domains of four EGF ligands in *D. melanogaster* and the EGF domain from the predicted Grk protein from *S. lebanonensis*; similarity with *D. melanogaster* Grk is shown in descending order. Black letters represent identical amino acids; blue letters represent amino acids with similar chemical properties; red letters represent amino acids that differ chemically. (b) Top, *D. melanogaster grk* gene locus and transcript (*grk-RA*); see (http://flybase.org/reports/FBgn0001137.html) for details. *S. lebanonensis grk* gene structure below. Gene structures are to scale. Colored boxes indicate homologous regions with the associated bit scores. (c) Schematic diagram of the construct used to test Grk^{Sl} activity in *D. melanogaster*.

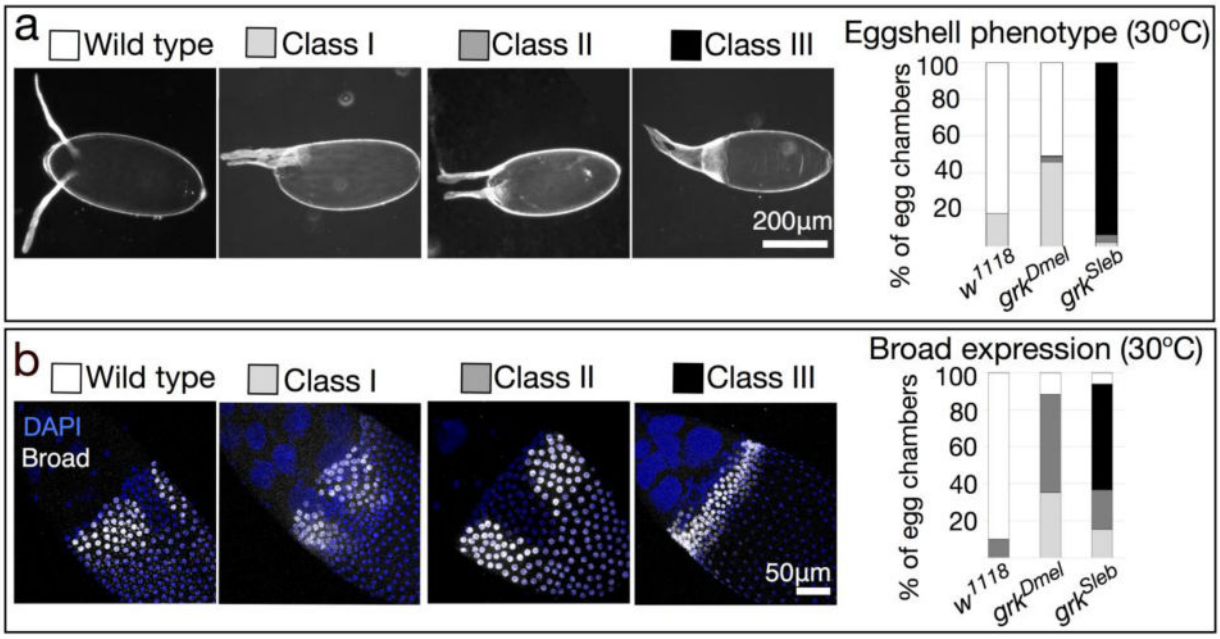

Fig. 8. *S. lebanonensis* Grk is active in a *D. melanogaster* background and alters tube- forming primordia

(a) Females were reared for 3 days at 30°C prior to egg collection. The *MTD-GAL4* driver (*G4*) is active in the germline at all stages of oogenesis. Representative images of eggshell phenotypes, in order of increasing degree of dorsalization: Wild type; Class I, having a single fused DA and/or ectopic DA material at the base; Class II, having an enlarged dorsal midline and laterally positioned DAs; Class III, having DA material completely surrounding the operculum. Anterior is to the left. Chart shows quantitation of phenotypic classes; N > 270 for each genotype. (b) Broad localizes to nuclei of follicle cells that will form the DA tubes at later stages. Representative images of Broad localization patterns: Wild type; Class I, having a narrow or absent midline; Class II, having an enlarged midline; Class III, having an expanded tube primordium around the circumference of the egg. Anterior is up and to the left. Chart shows quantitation of phenotypic classes; N ≥ 10 for each genotype.

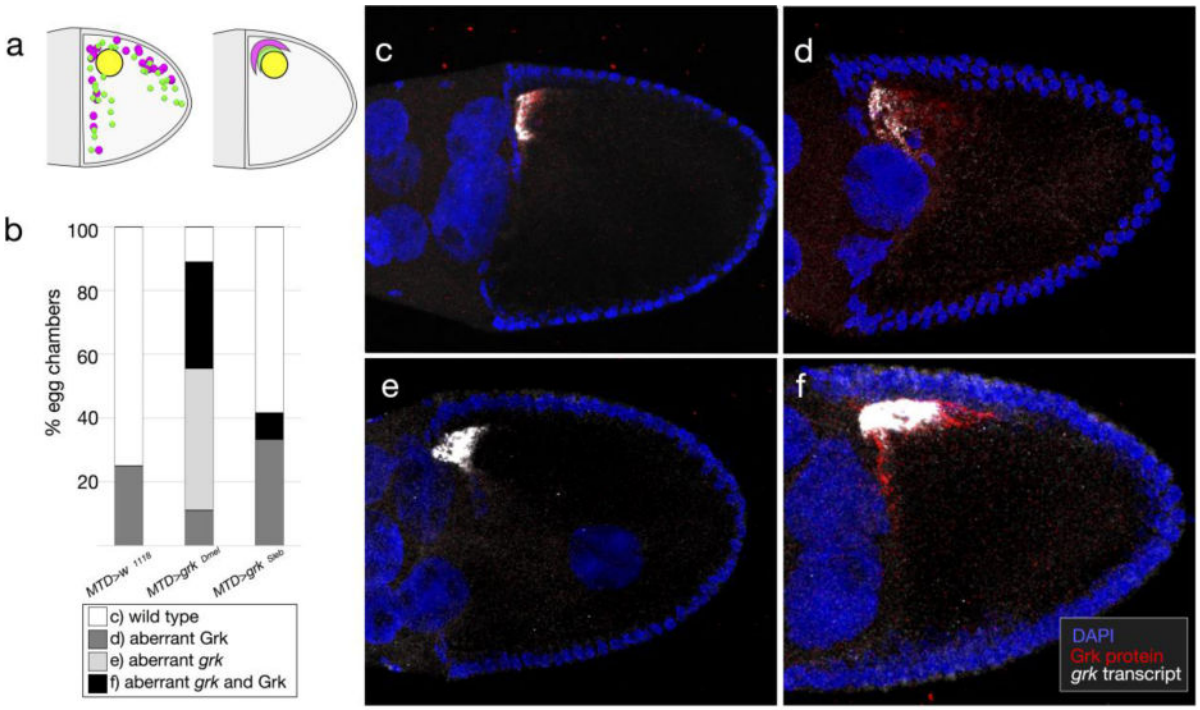

Fig. 9. IF/FISH demonstrates that expression of *S. lebanonensis* Grk does not mislocalize endogenous *gurken* protein or transcript

(a) Two hypotheses predict different localization patterns of endogenous *D. melanogaster gurken* protein and transcript in the presence of grk^{Sl}. Left: aberrant eggshells result from mis- localization of endogenous *grk* RNA or protein due to competition for regulatory factors with the introduced grk^{Sl} transgene products. Right: aberrant eggshell structures result from high activity of the introduced grk^{Sl} transgene. (b) Chart shows quantitation of phenotypic classes; N ≥ 10 for each genotype. (c-e) Representative images of phenotypic classes: (c) wild-type localization of *grk* transcript and Grk protein to the anterodorsal corner of the oocyte; (d) mislocalized and/or high levels of Grk protein, with wild-type *grk* transcript localization; (e) mislocalized and/or high levels of *grk* transcript, with wild-type Grk protein; (f) both mislocalized and/or high levels of *grk* transcript and Grk protein. Images show a lateral orientation with anterior to the left and dorsal up.

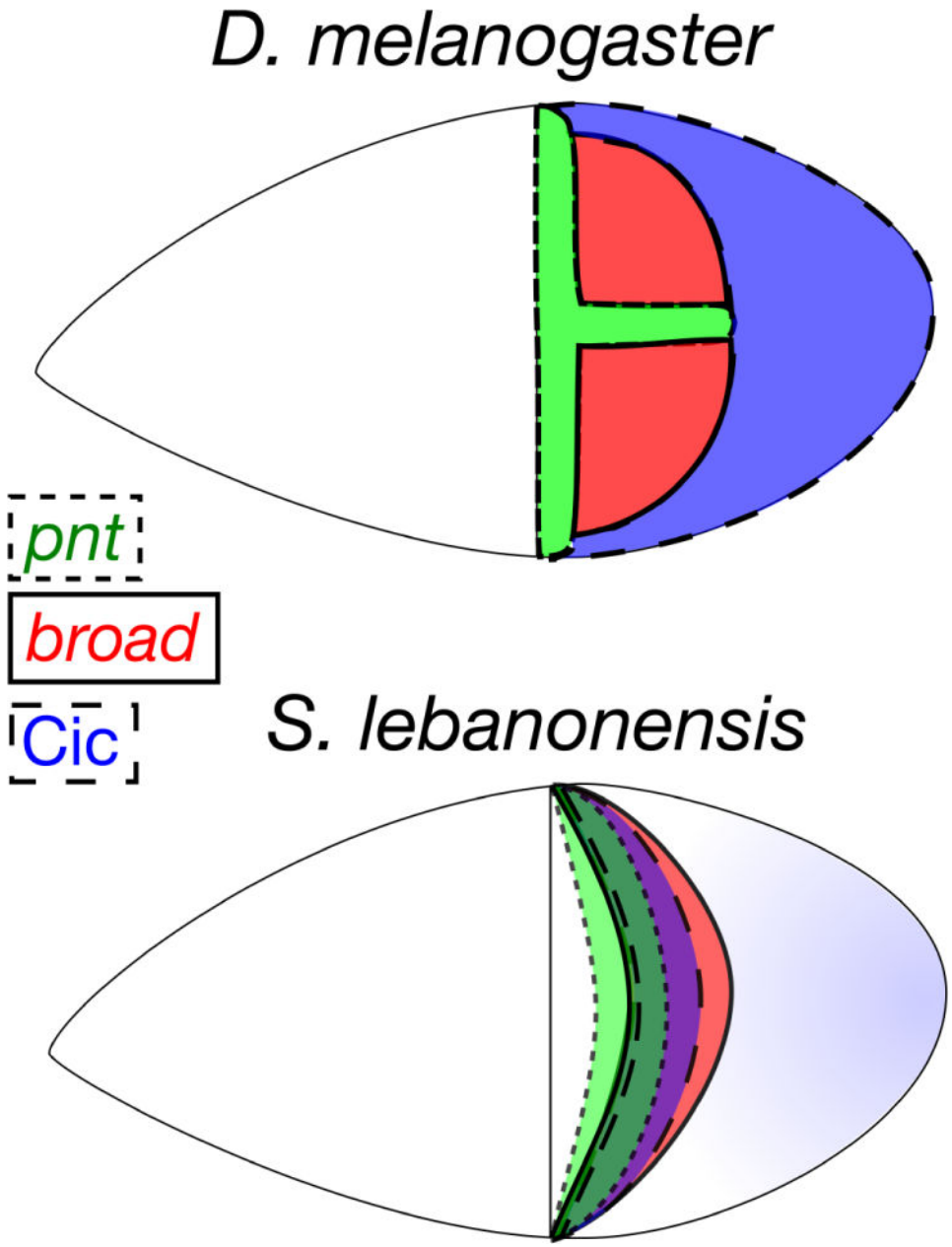

Fig. 10. A comparison of DA-primordia patterning in *D. melanogaster* and *S. lebanonensis*

Top: At S10B, *D. melanogaster* egg chambers express cell-type-specific markers in discrete, non-overlapping domains: *pnt* (green, midline), *broad* (red, DA roof cells), and Cic (blue, main body cells). Bottom: At S10B in *S. lebanonensis*, these markers overlap in a dorsolateral band: *pnt* (green region bounded by a dotted line), *broad* (red region bounded by a solid line), Cic (blue region bounded by a dashed line). Dark green (*pnt*, *broad*, and Cic) and purple (*broad*, Cic) regions illustrate where these transcription factors overlap.